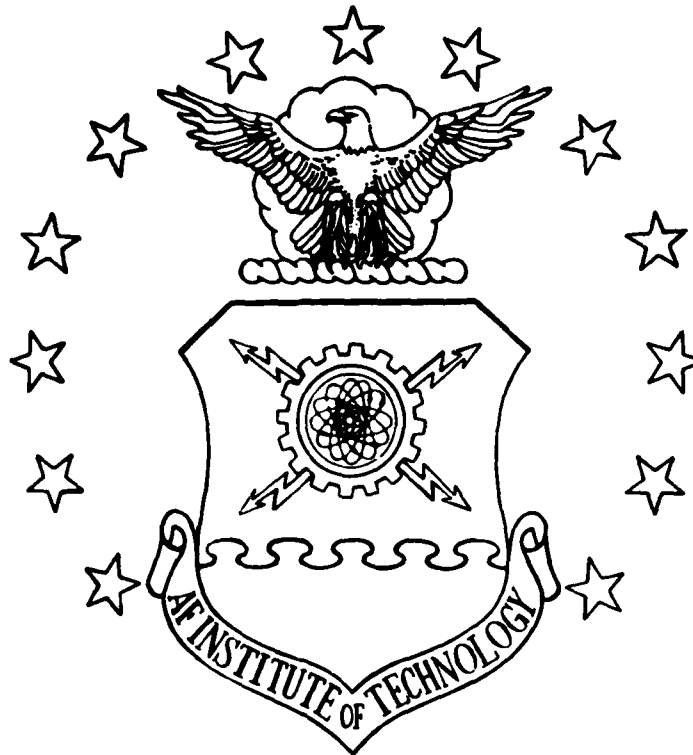


MICROCOPY RESOLUTION TEST CHART
NATIONAL BUREAU OF STANDARDS-1963-A

1

AD-A151 772



Dall-Null Tester for
Spaceborne Applications

Thesis

Randy L. Wingler
Captain, USAF

AFIT/GEP/PH/84D-14

DTIC FILE COPY

DISTRIBUTION STATEMENT A
Approved for public release;
Distribution Unlimited

DTIC
ELECTE
MAR 28 1985
B

DEPARTMENT OF THE AIR FORCE
AIR UNIVERSITY
AIR FORCE INSTITUTE OF TECHNOLOGY

Wright-Patterson Air Force Base, Ohio

85 03 13 150

AFIT/GEP/PH/84D-14

Dall-Null Tester for
Spaceborne Applications

Thesis

Randy L. Wingler
Captain, USAF

AFIT/GEP/PH/84D-14

DTIC
SELECTE
MAR 28 1985

B

DISTRIBUTION STATEMENT A

Approved for public release;
Distribution Unlimited

AFIT/GEP/PH/84D-14

Dall-Null Tester for Spaceborne Applications

Thesis

Presented to the Faculty of the School of Engineering
of the Air Force Institute of Technology

Air University

In Partial Fulfillment of the
Requirements for the Degree of
Master of Science in Engineering Physics

Rand. L. Minton, B.S.

October, 1984

AFIT-84-14

Approved for Release by NSA on 05-08-2014 pursuant to E.O. 13526

Table of Contents

	Page
Preface.....	I
List of Figures.....	II
Abstract.....	III
I. Introduction and background.....	1
II. Theory of the Foucault Test.....	7
III. Experiment to Produce a Foucault graph.....	22
IV. The Design of a Dall-Null system.....	29
V. Conclusions and Recommendations.....	43
Appendix A: Computer Program in Basic to solve for the Error in the Mirror's Surface.....	45
Appendix B: A Sample output From the Computer Program	54
Bibliography.....	59
Vita.....	65



Accession For	
NTIS	<input checked="" type="checkbox"/>
DTIC	<input type="checkbox"/>
Unannounced	<input type="checkbox"/>
Distribution/	
Availability Codes	
Dist	Avail and/or Special
A-1	

Preface

The purpose of this study was to design an adaptive optic system for a space based telescope. The design is built around a Dall-Kull tester. Much of the fine detail of the system was not researched because of the great difficulty and time required to correct all of the previous theory on which the design is based. However, the basis of a complete system is covered.

The making of the Focogram in the experimental section was very enjoyable and a nice break from the pitfalls of straight theory work. The results from the experiment showed the errors of the previous theories and paved the way to correcting them.

Several people have assisted me in this project. They are my adviser Dr. Dean Shadland, who always kept me headed in the right direction, but made me look and question every bend along the way; Paul Y. Curtis, the librarian who tracked down all the references that I requested; my class mate, Gregory Tarr, who wrote the tips on computer programming and handling the project; Curtis Tarr, who helped me gather and use the data on the project; and the other members of the team, who helped me in many ways. I would like to thank them all for their help and support. I would also like to thank my family, especially my mother, for their love and support. I would like to thank my friends, especially my friends at the University of California, for their love and support. I would like to thank my friends at the University of California, for their love and support.

List of Figures

Figure	Page
1. The basic layout of a Dall-Null tester.....	4
2. Notation reference for Welford's equations.....	14
3. Orientation for the application of Huygen's Principle.....	15
4. The Airy patterns making up the image of the pin hole.....	18
5. Mirror divided into four segments.....	19
6. The relative position of the Airy patterns at the knife-edge.....	20
7. The image of the mirror.....	21
8. Experimental setup with the HeNe Laser.....	22
9. Foucault results from the HeNe laser.....	23
10. Foucault results from the HeNe laser.....	24
11. Experimental setup with the white light source...	24
12. Foucault results from the white light source.....	25
13. Experimental setup with the sodium source.....	26
14. Foucault results from the sodium source.....	27
15. Notation reference for calculating the slope of the mirror.....	28
16. The graphed output from the mirror on the X-axis	36
17. Plot chart of the output from the mirror.....	37
18a. Configuration of the graph chart.....	38
18b. Configuration of the graph chart.....	39
19. Configuration of the graph chart.....	40
20. Configuration of the graph chart.....	41
21. Configuration of the graph chart.....	42

Abstract

This is a study to design a self-correcting primary mirror system for a space telescope. The design is centered around a Dall-Null tester (a Foucault knife-edge tester with compensating lens). An in-depth study of the theory of the Foucault test from Foucault's original publications to current work is presented. Also shortcomings of the diffraction approach are shown. The findings of a simple experiment showed the way to the correct explanation as to the workings of the test. Based on this new explanation, a computer program to find the error in the surface of the mirror from the irradiance pattern provided by the Dall-Null tester was developed. The computer program with a sample run is included in the appendixes A and B.

The basic design of an adaptive optic system for a space-borne application is also presented in the paper. This design has the desired quality of being able to correct the mirror while the telescope is in use. The equations being independent of wavelength allow the design to be applied to systems which cover a wide range of wavelengths such as the system which is being designed.

Chapter 1

Introduction and Background

Ever since Galileo turned his telescope to the heavens, man has tried to improve this sky gazing instrument in order to gain more information from the skies. The best improvement that can be made in any telescope is to increase its light gathering capabilities. Increasing the size and improving the quality of the main optical element are the easiest ways to improve the light gathering capability of a telescope. The primary, or main optical element in a reflecting telescope, is the main mirror. And in a refracting telescope it is the large first lens. Since most large telescopes are reflectors, due mainly to more compact size and the lighter weight of the system, this paper will concern itself with improvements that are more suitable for reflecting telescopes.

Increasing the size of the primary mirror in a telescope is the only way of increasing the light gathering capability. However, this has drawbacks, for it may be either impractical or impossible to make a larger telescope. Therefore, it is desirable to have a way to improve the light gathering capability of a telescope without increasing its size. This is the purpose of this paper. It is a study of the possibilities of improving the light gathering capability of a reflecting telescope by the use of a secondary mirror. The secondary mirror is placed in the light path between the primary mirror and the eyepiece. This secondary mirror is used to reflect the light from the primary mirror to the eyepiece. This is done in such a way that the light from the primary mirror is focused on the eyepiece. This is the principle of the Cassegrain telescope. The secondary mirror is usually a convex mirror, and the primary mirror is a concave mirror. The secondary mirror is placed at a distance from the primary mirror such that the light from the primary mirror is focused on the eyepiece. This is the principle of the Cassegrain telescope. The secondary mirror is usually a convex mirror, and the primary mirror is a concave mirror. The secondary mirror is placed at a distance from the primary mirror such that the light from the primary mirror is focused on the eyepiece. This is the principle of the Cassegrain telescope.

It is the reflective coating on the surface of the mirror that determines the reflectivity of the mirror. Therefore, any improvement in the reflectivity of the mirror is limited to the thickness and type of coating applied. Since the reflectivity is set in this manner, the only way left to improve the quality is to rid the surface of the mirror of defects. Most surface defects or imperfections are removed while the mirror is being fabricated.

Optical telescope mirrors are made by grinding glass into the desired shape and then coating them with a highly reflecting substance, like silver. As the glass is ground into the desired shape it is visually monitored for defects and imperfections. The most commonly used test for checking the mirror is the Foucault knife-edge test (or one of its derivatives). The Foucault test has one large deficiency. It was designed to check only spherical surfaces and not parabolic surfaces. But parabolic surfaces are the standard used to check all reflecting surfaces, including periscopes, binoculars, and the optical systems of cameras. It is therefore necessary to use a method to check the quality of a parabolic surface.

The method used to check the quality of a parabolic surface is the Ronchi test. The Ronchi test is a simple test that can be performed in a dark room. It is a variation of the Foucault test. The Ronchi test is a simple test that can be performed in a dark room. It is a variation of the Foucault test.

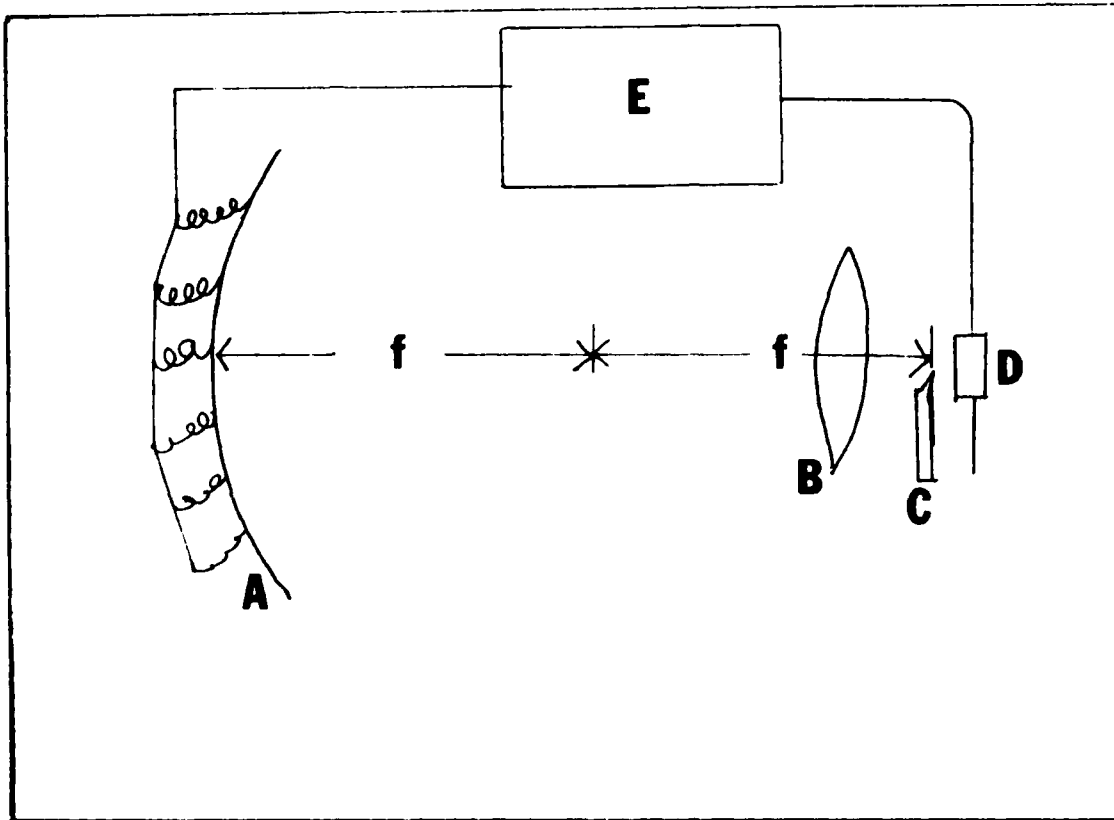


Figure 1 The basic layout of a Dall-Null tester
 A is the deformable mirror with attached actuators
 B is the compensating lens
 C is the knife-edge
 D is the detector for reading the irradiance
 E is the computer and other electronic equipment

to escape the atmospheric limitations. This does cause some problems. One such problem is, "How can the surface of the mirror be tested to see if it has been twisted and warped out of shape by thermal and gravitational gradients as it spins around the earth?". This leads to the second question, "If surface defects do occur, how are they detected and corrected?".

One way to answer both of the above questions is to make the telescope with an adaptive optics system. This adaptive optics system consists of the following: a deformable main mirror with actuators, a computer, some electronics, a Dall compensating lens, and two Foucault testers. Figure 1 shows the basic layout of an adaptive optics system of a telescope. The deformable mirror is made by shaping a semiflexible material into the desired shape, and then coating it with a highly reflective substance (17,28). Then actuators (devices that can apply a push or pull force) are mounted on the back surface of the mirror. There are two major types of actuators. The first is the force type that uses either a stepping motor, or an electrodynamic voice coil to generate a push/pull force. The second is the piezoelectric type that contracts or expands with applied voltage (1). The computer's job is to calculate the error of the surface of the mirror from the irradiance of the images caused by each of the Foucault testers, and then to take the error information and correct the surface of the mirror through movement of the actuators. Two Foucault testers are needed to produce both a vertical and a horizontal scan. The two knife-edges are located approximately at the center of curvature, but orientated at 90 degrees from each other. The proper Dall compensating lens corrects the Foucault test for parabolic surfaces (6,7). The additional electronic equipment needed to complete a system consists of a sensor to read the irradiance, equipment to digitize the irradiance

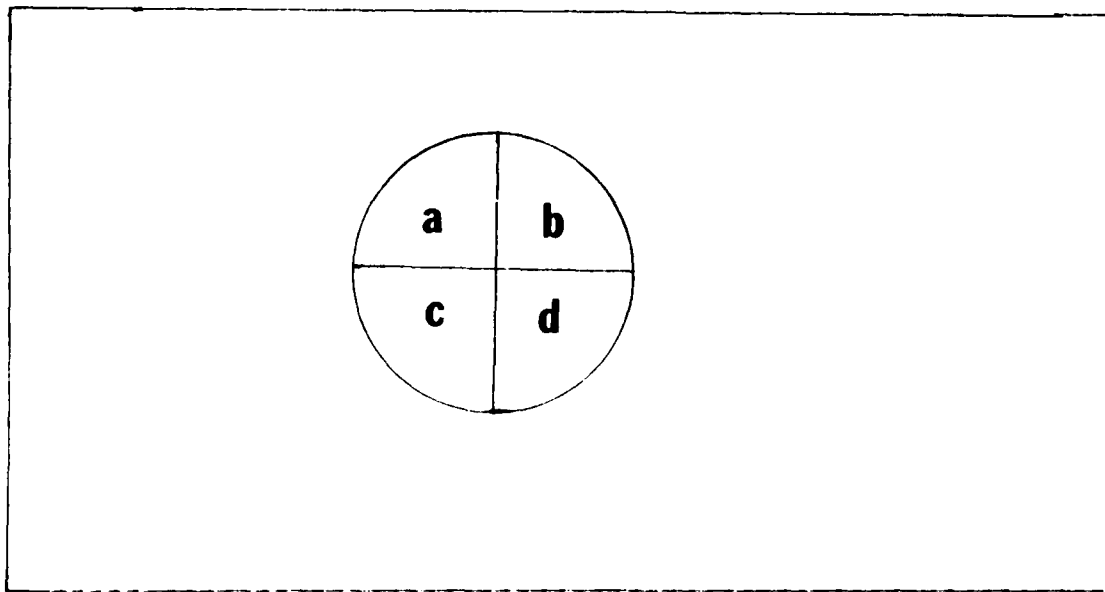


Figure 5. Mirror divided into four segments

pattern that is small ($\approx \lambda$). (Figure 4). These Airy patterns would either be passed by the knife-edge, or stopped completely, with just a few patterns left to straddle the knife-edge. It is these straddling patterns that would produce the effect of equation (2). But, because the light is incoherent, the irradiance of the waves add and not just their fields. This removes the singularities.

Now if the mirror was segmented into sections, as in Figure 5, each segment having a different local slope, the position of the light at the focus would be determined by the slope of each segment. Figure 6 shows the relative position of the light from each segment of the mirror relative to the knife-edge. If the slope is that of a perfect surface the knife-edge would split the image, case b, passing half and stopping half. If the slope was such that it raised the

$A(\underline{x})$ = the aperture function

$$\underline{x} = (x_1, x_2)$$

$$\underline{y} = (y_1, y_2)$$

$$\underline{z} = (z_1, z_2)$$

b = the distance the knife is displaced from the optic axis

But when equation 2 is used (being careful in expanding out all transforms and exponentials) to relate the irradiance of the image to the errors of the mirror, the resulting equations are so messy and complex they can not be solved. This is one of reasons the experiment described in chapter three was conducted.

The experiment described in Chapter Three was performed to verify what kind of results are obtained from an actual Foucault test, and to examine some of the operating parameters. The results of the experiment showed no existence of a bright rim around the image, and that the aperture did not affect the image at the screen as long as it does not intersect the beam. The experiment also showed that the light source had to be incoherent, and that monochromatic light was better than plain white for testing lenses due to the different focal length of each wavelength.

When using the laser as the source of radiation in the experiment, it became apparent that the diffraction theory of the Foucault test was inadequate to describe the results.

Where a = slit width

$$= M\lambda R/b$$

$$n^\circ = m\lambda R/b$$

b = pupil radius

M = number of Airy patterns across slit

m = number of Airy patterns the lower edge is displaced from the center of the image

R = the radius out to the image from the knife-edge

λ = wavelength

The only real difference between this equation and that of Linfoot's is that the factor $1/(y-y')$ which gave the singularity is now replaced by the sine function which has no singularity.

Melford's equation is basically the same result that the author, working in conjunction with Dr. Shankland, obtained upon applying Huygens' principle to the problem, (Figure 3). The resulting equation for the complex amplitude, $P(\underline{x})$, is

$$P(\underline{x}) = B \int_{-\infty}^{\infty} K(\underline{x}, \underline{x}') U(\underline{x}') \quad (2)$$

where

$$K(\underline{x}, \underline{x}') = \int_{-\infty}^{\infty} \exp(-ikz) \exp(i\sqrt{k^2 - \xi^2} z) \exp(i\xi(x-x')) \exp(i\xi(x'-x')) \exp(-i2\pi \xi y / \lambda R)$$

$$B = (0.5)^{1/2}$$

$$k = 2\pi / \lambda$$

$$L = \text{distance from slit to pupil}$$

$$M = \text{number of Airy patterns across slit}$$

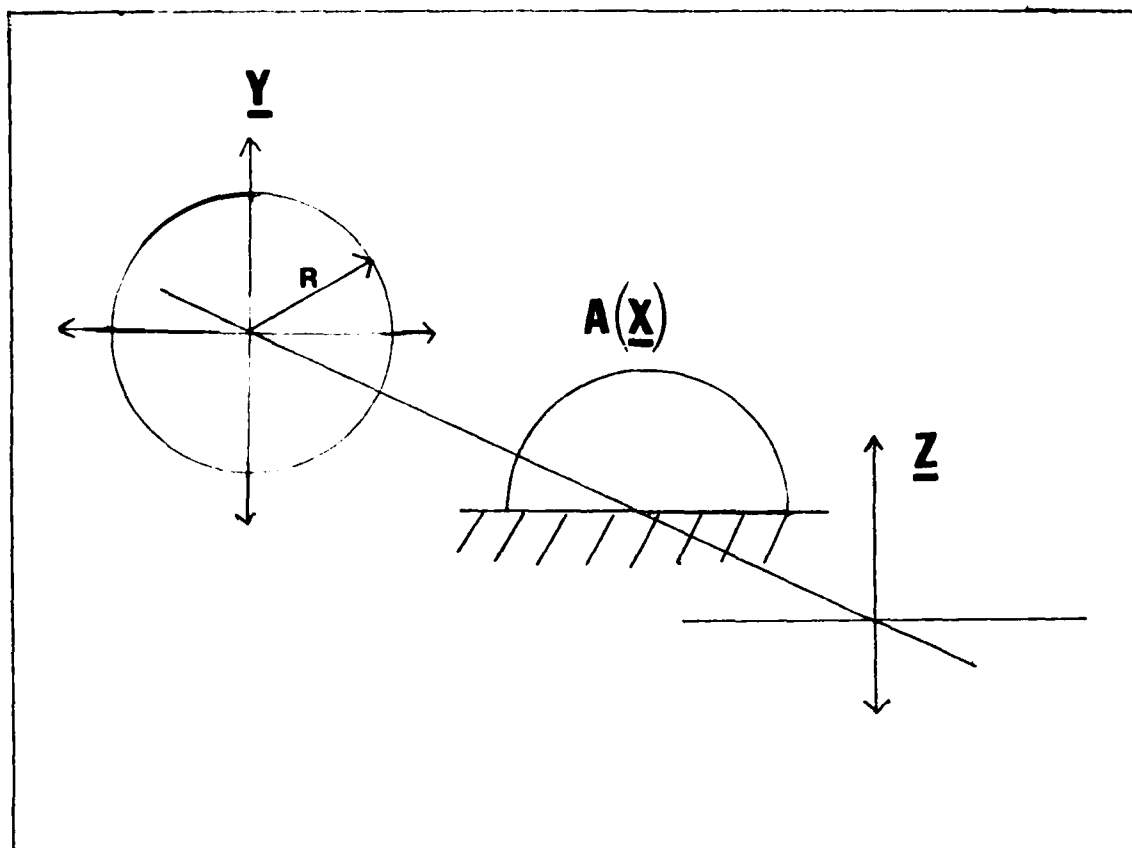


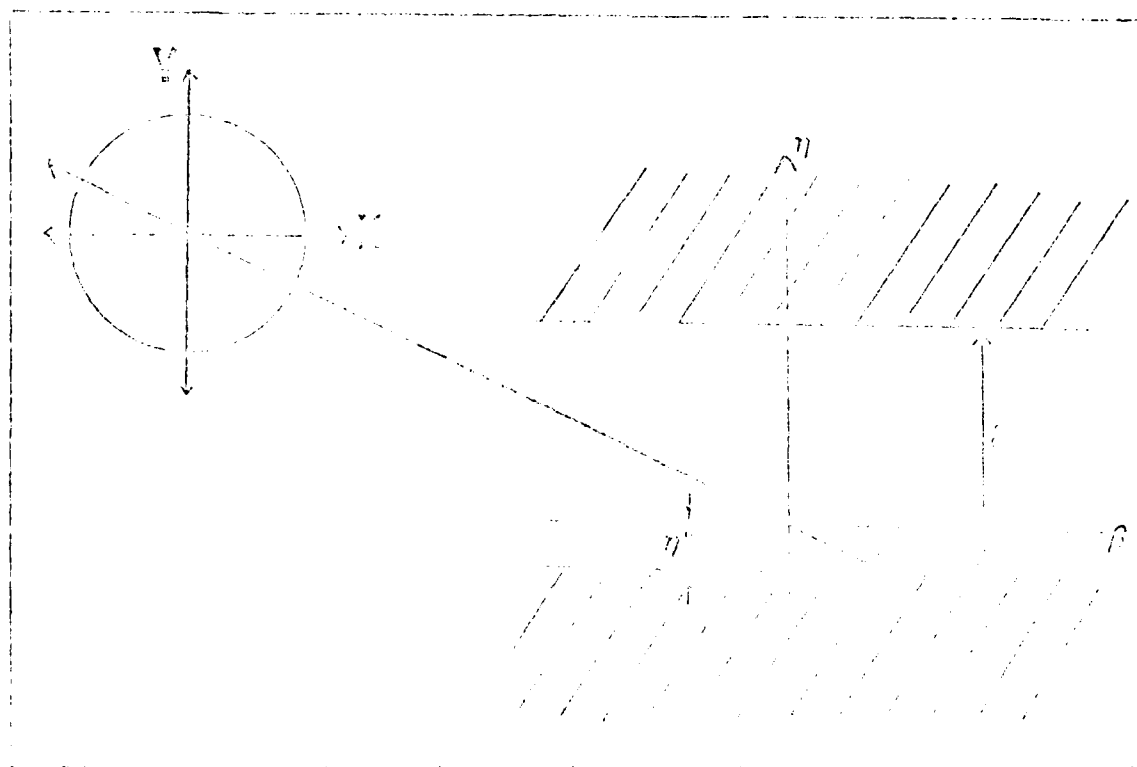
Figure 3 Orientation for the application of Huygens' Principle

disregard it as there could not be an actual infinity in the complex amplitude. Linfoot said that this infinity was due to the assumption of an infinite aperture. Welford decided to test this, and rederived Linfoot's work with a proper aperture function included. He used a very wide slit in the place of the knife-edge. Using Figure 2 as a reference, the equation Welford derived for the complex amplitude is:

$$U(x', y') = \int_{-\infty}^{\infty} a \operatorname{sinc}(M/b(y-y')) \exp(-\pi i/b(M+2m)(y-y')) F(x', y) dy$$

A plot of the perfect mirror's irradiance is found on page 140 of reference 23, and the plot of the perfect cassegrain mirror is on page 141. The point to note here is that the graphs and theory predict irradiance well out into the surrounding area outside of the mirror's boundary. This is not observed in practice.

W. T. Welford wrote an article (33) on the theory of the Foucault test in 1970, in which he noted that in Linfoot's, and his predecessors', computations a bright rim was predicted around the edge of the pupil of the system under test. Users of the test do not observe this bright ring, and



using a one inch diameter lens to expand the image; the "sec" term is less than one part in 100,000 at the edge of τ , where τ in this case is the semicircular edge corresponding to the value of $[u^2 + v^2]^{1/2}$ which is approximately 1300 (inch).⁻¹ Disregarding the effects of the finite aperture of the viewing system, one can replace τ with infinity as the image is defined to be zero outside of the mirror. The complex amplitude now can be written,

$$D(x', y') = \frac{1}{2\pi} \int_0^\omega du \int_{-\omega}^\omega \exp(-iux' - ivy') W(u, v) dv$$

This reduces to the expression:

$$2\pi D(x', y') = \pi D(x', y') + i \int_{-\omega}^\omega \frac{W(u, y')}{i - u'} du$$

and the observed irradiance is:

$$I(x', y') = 2\pi^2 \left| D(x', y') \right|^2$$

The error of this approximation is:

$$I(x', y') = 2\pi^2 \left| \left[D(x', y') + \frac{i}{2\pi} \int_{-\omega}^\omega \frac{W(u, y')}{i - u'} du \right] \right|^2$$

This is saying the irradiance is uniform across the surface and zero outside the boundary of the mirror. If the surface of the actual mirror surface is labeled M , which is within a few wavelengths of a true spherical surface labeled M^0 , then the wave at any point (x,y) is:

$$E(x,y) = |E(x,y)| \exp((-2\pi i/\lambda) \theta(x,y))$$

where $|E(x,y)|$ = the amplitude at the point (x,y)

$\theta(x,y)$ = the phase at the point (x,y)

λ = the wavelength

Now applying Huygens' principle along with the Paraxial approximation twice, once to the half-edge and again to the image, results in the equation for the complex amplitude (the square of the amplitude is the irradiance) as:

$$U(x',y') = \frac{1}{2\pi} \int_{\Sigma} \exp(-i\pi x' u - i\pi y' v) V(u,v) \exp\left(\frac{i\pi}{2\lambda} (u^2 + v^2)\right) du dv$$

$$\text{where } u = 2x/\lambda$$

$$v = 2y/\lambda$$

Σ = the surface of the mirror, $V(u,v)$ the field over Σ

$$V(u,v) = \frac{1}{\lambda^2} \int_{-\infty}^{\infty} \int_{-\infty}^{\infty} V(x,y) \exp(i\pi(xu + yv)) dx dy$$

... ..

Where R is some retardation function

x = the position out from the center

(the radius has been normalized to one and y is just a variable of integration)

In the case of the perfect mirror, the retardation function, R, is equal to zero everywhere, and the equation reduces to Rayleigh's result, infinity at the edge of the mirror.

S. C. B. Gascoigne, working with H. U. Linfoot, took Zernike's work as his starting point and derived expressions for the irradiance that are valid for errors of arbitrary form and amount, in terms of definite integrals (Hilbert transforms). Gascoigne's equation for the irradiance of a perfect mirror is equivalent to Zernike's (equation 1). Gascoigne has tabulated his irradiance results on page 332 of reference 12 and plotted the results on page 334 of same reference.

It wasn't until Linfoot published his work in 1955, before anyone worked out the theory completely in two or more dimensions (23). The case of a plane wave incident under uniform illumination in which the error in the mirror could be expressed as:

$$f(x,y) = 1 \quad \text{for } (x,y) \text{ inside } (1)$$

$$= 0 \quad \text{for } (x,y) \text{ outside } (1)$$

A151772

was well out of the focal plane. His calculated irradiance ratios were then matched against photographic observed ratios with less than ten percent difference between corresponding points. Thus, Rayleigh's theory stood its ground, untouched until 1934.

In 1934, professor F. Zernike published his diffraction theory of the Foucault test(35). Zernike felt that the geometrical optic approach to the Foucault test did explain things well enough for the lens grinder to find the spots where more grinding was necessary, but in a test where wavelength defects could be detected, only wave optics and diffraction could completely describe the actual happenings and give the test's ultimate limit of sensitivity (35:377). He envisioned the surface of the mirror as a diffraction grating that would give first order spectra on both sides of the central image, which he called a phase grating. He built up his work by expressing everything in terms of this phase grating. From his phase grating expressions, he developed what is now called the method of phase contrast. This phase contrast method assigns phases to the different shades of irradiance in the image. Zernike's equation for the observed intensity, $I(x)$, is:

$$I(x) = \pi^2 + \ln^2 \left| \frac{1-x}{1+x} \right| - 2\pi \int_{-1}^1 \frac{R(y) - R(x)}{y-x} dy \quad (1)$$

$$I(x) = \frac{2}{\pi} + \ln^2 \left| \frac{D-x}{D+x} \right|$$

for the irradiance inside the edge of the mirror and

$$I(x) = \ln^2 \left| \frac{D-x}{D+x} \right|$$

for the irradiance outside the edge,

where D = the radius of the mirror

x = the position out from the center

At the edge of the mirror, when $x = D$, the logarithmic infinity that results is what Rayleigh said accounted for the bright ring around the image.

Sudhansukumar Banerji, in 1918, wrote that he had observed irradiance fluctuations of the entire surface when the knife-edge was considerably advanced and that there were no known repetitions or explanations of this effect (2). He then proceeded to show that the fluctuations could be explained using aperture theory. Banerji then pointed out that Rayleigh had confirmed his findings in the case where the knife-edge was exactly at the focus and in particular, the position of the screen did not depend on the distance and could be regarded as a constant. He also pointed out that the fluctuations could be explained by the fact that the aperture was not perfectly circular and that the fluctuations were due to the fact that the aperture was not perfectly circular and that the fluctuations were due to the fact that the aperture was not perfectly circular.

bright ring about the edge. The model also accounted for the bright line which appears at a step-discontinuity on the mirror surface.(27)

The theory of the Foucault test, as developed by Lord Rayleigh, gives irradiance of the field for the general case of any mirror, as viewed in the direction θ (relative to the optic axis) in terms of the Fresnel Cosine (Ci) and Sine (Si) integrals as:

$$I = \left[\text{Si} \left[\frac{2\pi}{\lambda} \beta (1 + \theta/\beta) \zeta_2 \right] - \text{Si} \left[\frac{2\pi}{\lambda} \beta (1 + \theta/\beta) \zeta_1 \right] + \text{Si} \left[\frac{2\pi}{\lambda} \beta (1 - \theta/\beta) \zeta_2 \right] - \text{Si} \left[\frac{2\pi}{\lambda} \beta (1 - \theta/\beta) \zeta_1 \right] \right]^2 + \left[\text{Ci} \left[\frac{2\pi}{\lambda} \beta (1 - \theta/\beta) \zeta_2 \right] - \text{Ci} \left[\frac{2\pi}{\lambda} \beta (1 - \theta/\beta) \zeta_1 \right] - \text{Ci} \left[\frac{2\pi}{\lambda} \beta (1 + \theta/\beta) \zeta_2 \right] + \text{Ci} \left[\frac{2\pi}{\lambda} \beta (1 + \theta/\beta) \zeta_1 \right] \right]^2$$

where λ = Wavelength

ζ_2 = upper limit of aperture

ζ_1 = lower limit of aperture

θ = angular semi-aperture of the lens under test

Applying Rayleigh's irradiance equation for the special case of a perfect spherical mirror, tested at the center of curvature, with a change of variable in order to do the integration, the above equation for $I(x)$ reduces to:

Chapter 2

The Theory of the Foucault Test

After 1858 and 1859, when Leon Foucault published the first accounts of the Foucault knife-edge test, it rapidly became the optical test to verify the surface condition of a lens or a mirror (9,10,25:231). His first article described how to conduct the test, how to interpret the results, but not how or why it works (9). In his second article, he did attempt to explain the happenings in terms of geometric ray optics (10). This explanation worked well for extremely large errors but did not account for all of the observed effects. As Linfoot pointed out, the effects that are produced by the small errors (on the order of one to ten wavelengths) often caused trouble for the inexperienced mirror/lens grinder (24:128). One of these errors is the bright ring around the image of a properly ground lens. According to Foucault's original work, this bright ring could only be explained by saying it represented a steep narrow-turned edge, but there is no such edge on the surface of a properly ground lens.

In 1917, Lord Baron Rayleigh made the first attempt to derive a complete theory of how and why the Foucault test worked based on diffraction theory and wave optics. He used a simplified two-dimensional model (all equations and work were in one dimension) which qualitatively explained the

of the images for the computer, and equipment to provide the feedback between the actuators and the computer. Chapter four will discuss how the error in the surface height of the mirror is calculated from the irradiance pattern.

The complete system, deformable mirror, actuators, Dall-Null tester, computer, and the computer software for reading the focogram and controlling the actuators, comprised the necessary equipment to make up a self-correcting mirror system for a space-borne telescope application. This system has one big advantage over other possible systems for telescope applications. It works at the center of curvature and not at the focus. This allows the testing and correcting of the primary mirror to occur while the telescope is in use.

Chapter five will present conclusions of this study with recommendations for further study, the possible uses of such an adaptive system in systems for space-borne telescopes, and possible future developments.



Figure 6. The relative position of the Ariy patterns at the knife-edge.

image, cases a and d, then all of the image will pass the knife-edge. But if the slope lowered the image, case c, the knife-edge would cut it off completely. Thus the irradiance of the resulting image would be determined by how much of each segment's image was passed by the knife-edge. Figure 7 shows the result for the current situation.

Thus the correct theory of the Foucault test is revealed, and likewise, so is the theory of the Dall-Null test. And in chapter four this theory will be put to work to find the error in the height of the mirror surface.

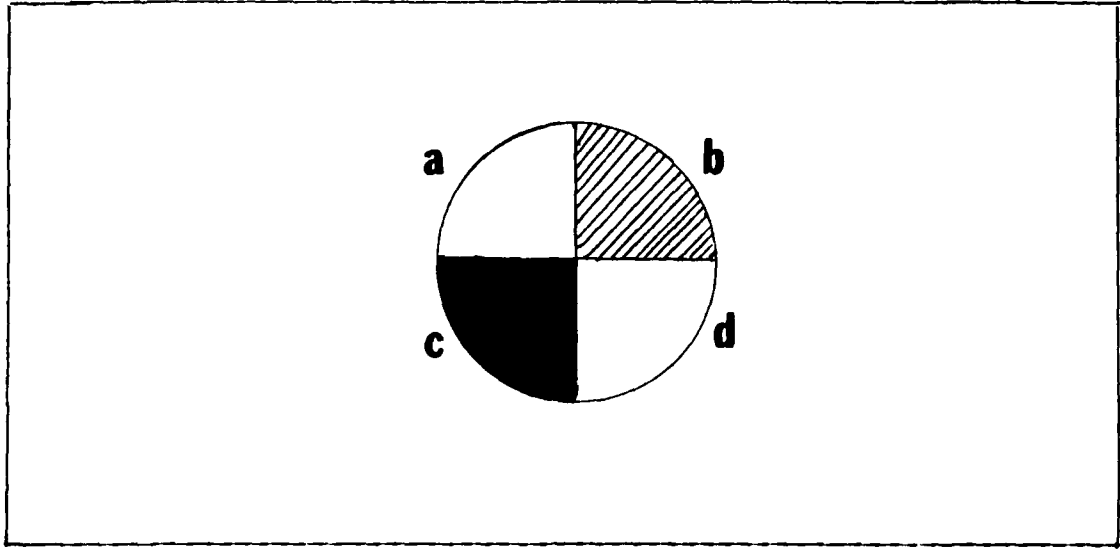


Figure 7. The image of the mirror

Chapter 3

An Experiment to Produce a Focogram

The Focograms presented in the literature (25:233-241, 20:390) did not show any bright rim about the edge that theory, according to Linfoot and his followers, says should be there. To answer the questions, "Is the theory right or is there something happening that is being missed?" and "Is Welford right in that it is the aperture function that will cure the infinity at the edge?", a simple experiment was set up to produce a Focogram of a lens.

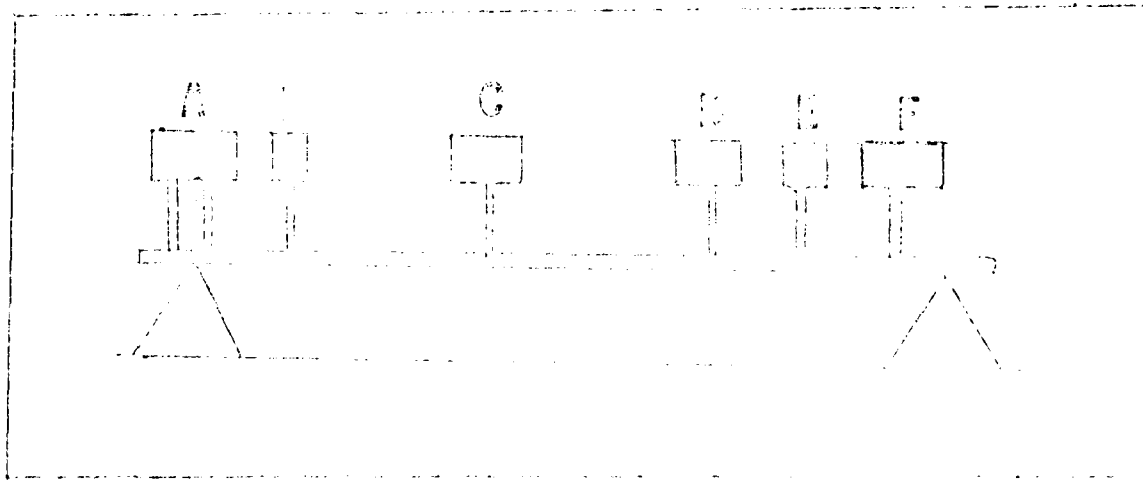


Figure 3. Schematic diagram of the experimental setup for producing a focogram of a lens. The lens A is the lens to be tested. The lens C is the lens used to focus the light on the film plane. The lens F is the lens used to focus the light on the detector. The components B, D, and E are used to control the light path and the aperture function.

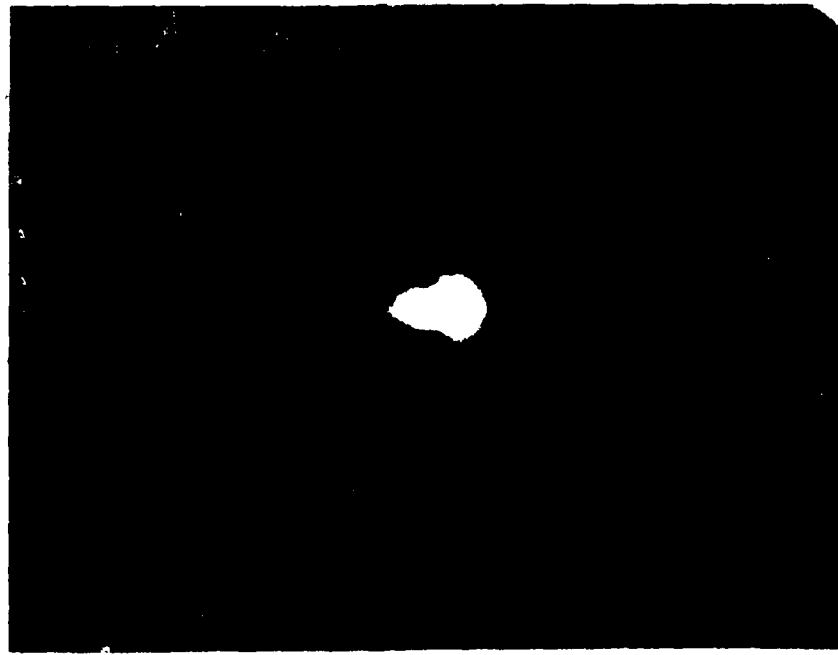


Figure 9. A dark, rectangular image with a small, irregular white shape in the center.

The image shows a dark, rectangular area with a small, irregular white shape in the center. This shape is likely a hole or a mark on a surface. The image is framed by a thin white border.



Figure 10 Foucault results from the HeNe laser

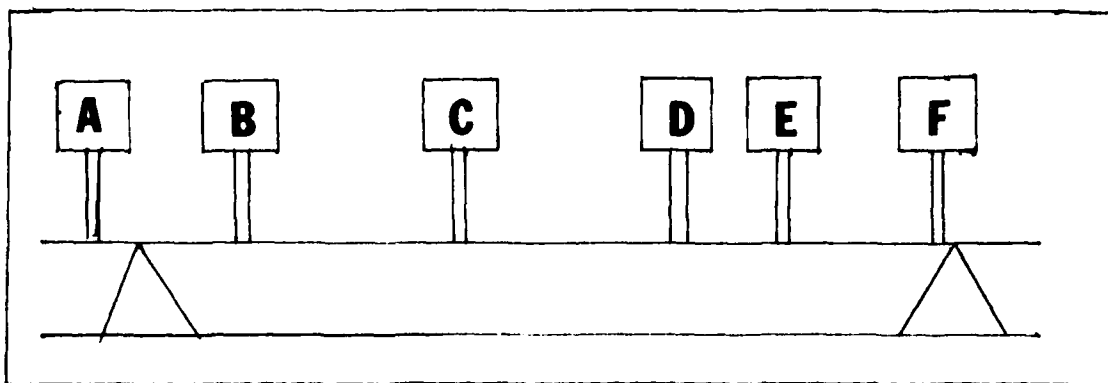


Figure 11 Experimental setup with the white light source
A is white light source
B is the pinhole
C is the lens under test
D is the knife-edge
E is the imaging lens
F is screen/camera

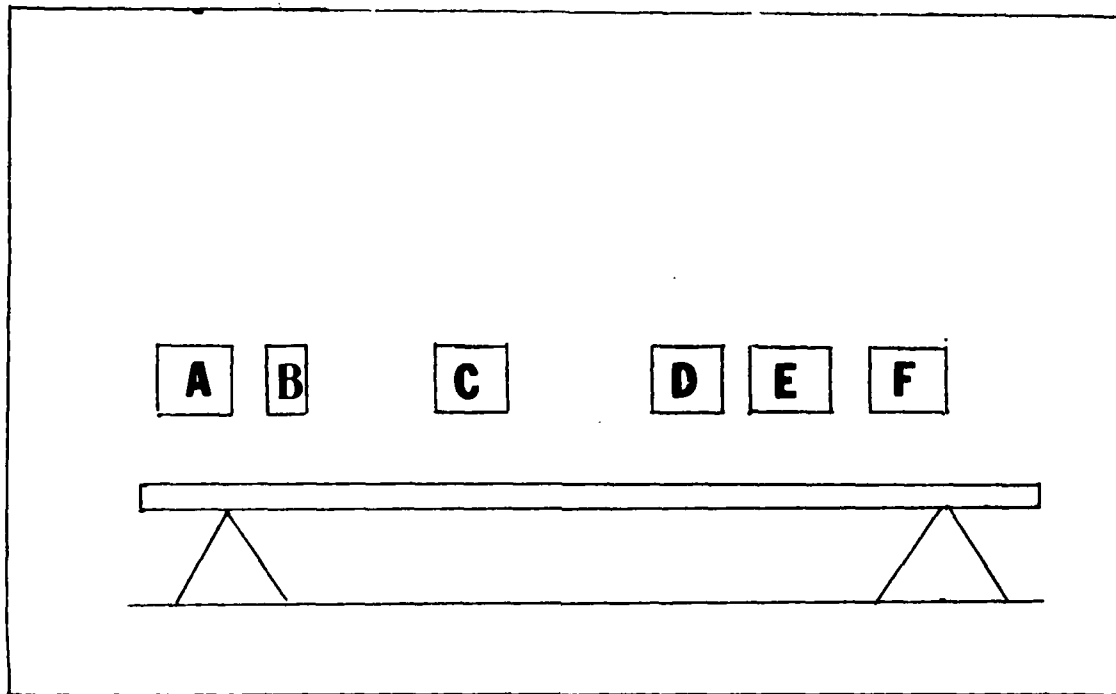
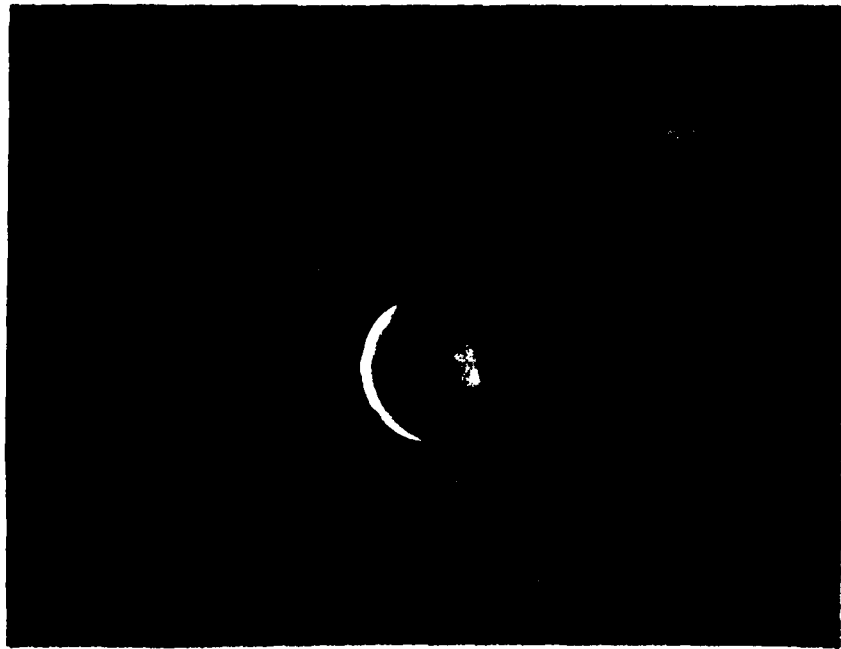


Figure 13 Experimental setup sodium source
 A is the sodium lamp
 B is the pin hole
 C is the lens under test
 D is the knife-edge
 E is the imaging lens
 F is the screen/camera

across the image at all times regardless of the amount of the beam the knife-edge cut off. The results that were obtained are presented in Figure 12.

The setup was then altered by the replacement of the white light source with a Sodium lamp as in Figure 13. The lenses' positions were adjusted for the wavelength with their order on the optic bench remaining the same. This setup gave the true Focogram that is presented as Figure 14.

A test to see how the aperture affects the image was conducted by inserting a 3 by 5 inch index card into the



the Foucault test. The actual explanation as to what is happening is presented in Chapter 2 pages 17-20.

Chapter 4

The Design a Ball-Bull Tester

To interpret the information from the Foucault graph in an adaptive optical system, the theory that is presented in chapter two is used as the starting point. Each of the images of the knife-edge is scanned to yield the irradiance as a function of x and y . The irradiance is then divided by the background irradiance and run through a transformation to obtain the slope of the mirror surface. This slope of the mirror surface is then integrated to yield the height of the surface. Then the square of the differences of the integrated height for each direction at each point (x,y) , is minimized to obtain the least least squares of the mirror's surface. The derivation of the equations to accomplish this task is as follows.

For a scan in the x -direction, the irradiance, $I(x)$, is seen from the knife-edge at the surface at x . $z(x)$ is the distance of the knife-edge from x to z , when $I(x) = I(z)$. The irradiance, $I(x)$, is given by

$$I(x) = I_0 \left(\frac{z}{R} \right)^2 \left(\frac{z}{R} - \frac{z^2}{R^2} \right)^2$$

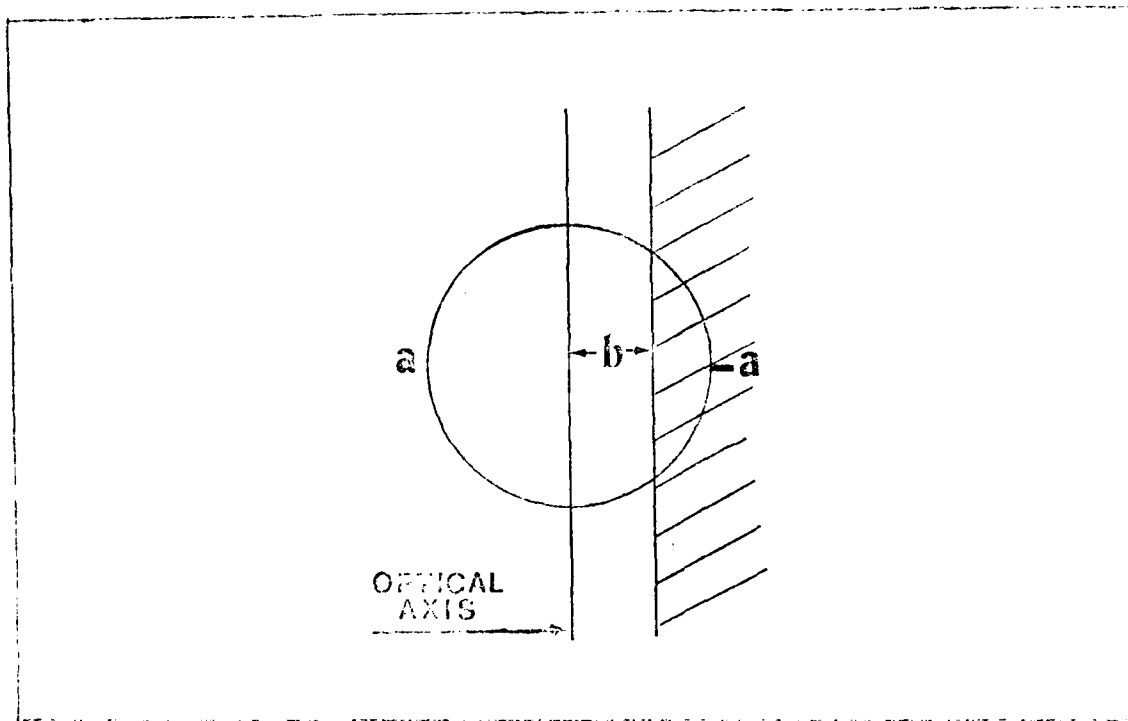


Figure 15. Geometric representation for calculating the slope of the line $u = u(x)$ at $x = 0$. a = radius of cylinder b = distance between left face of and center of cylinder

$$u = 2a \int_{-a}^a \frac{G(x)}{2a^2 - x^2} dx$$

$$u = 2a \int_{-a}^a \frac{G(x)}{2a^2 - x^2} dx$$

where $G(x) = \frac{1}{2} \rho(x) u(x)$

$$G(x) = \frac{1}{2} \rho(x) u(x)$$

where $\rho(x)$ is the density

$$\rho(x) = \frac{1}{2} \rho(x)$$

where $b = 2Lm(x)$

L = distance between the mirror and knife-edge

$m(x)$ = the local slope of the mirror

The irradiance, $I(x)$, is then:

$$I(x) = I_0 A \\ = I_0 (\pi/2 + \arcsin(b/a) - (b/a)(1 - (b/a)^2)^{1/2})$$

where I_0 is the background irradiance.

Replacing b with $2Lm(x)$ yields:

$$I(x)/I_0 = \pi/2 + \arcsin(2Lm(x)/a) - (2Lm(x)/a)(1 - (2Lm(x)/a)^2)^{1/2}$$

Since the y value has been a constant all through this development, and implied, it can be inserted as a part of the final equation to give:

$$I(x,y)/I_0 = \pi/2 + \arcsin(2Lm(x,y)/a) - (2Lm(x,y)/a)(1 - (2Lm(x,y)/a)^2)^{1/2}$$

As the y value is constant, L is constant, so L can be moved with the a value, $M(x,y)$, thereby yielding the varying variable $M(x,y)$ as the only variable in the equation.

$$I(x,y)/I_0 = \pi/2 + \arcsin(2M(x,y)/a) - (2M(x,y)/a)(1 - (2M(x,y)/a)^2)^{1/2}$$

where $M(x,y) = Lm(x,y)$

$M(x,y)$ = the local slope of the mirror multiplied by the distance between the mirror and knife-edge

$$m(x, y) = dh(x, y)/dx$$

$$n(x, y) = dh(x, y)/dy$$

$$h'(x, y) = \int_0^x m(x', y) dx' + f(y)$$

$$h''(x, y) = \int_0^y n(x, y') dy' + g(x)$$

The mean difference squared between the slopes for each spot, S , can only be minimized by varying the functions $f(y)$ and $g(x)$ in the equation:

$$S = \frac{1}{N} \int_0^1 \int_0^1 (m'(x, y) - h''(x, y))^2 dx dy$$

$$m'(x, y) = \int_0^x m(x', y) dx'$$

$$n'(x, y) = \int_0^y n(x, y') dy'$$

$$m'(x, y) = \int_0^x \int_0^y m(x', y') dx' dy' + f(y)$$

So that

$$\delta S / \delta \mu = 0 \quad \text{when evaluated at } \mu = 0$$

$$= \int_0^a dx dy (h'(x, y) - h''(s, y)) \tau(y)$$

$$\delta S / \delta \beta = 0 \quad \text{when evaluated at } \beta = 0$$

$$= \int_0^a dx dy (h'(x, y) - h''(x, y)) \mu(x)$$

$$0 = \int dy \tau(y) \int_0^a dx (h'(x, y) - h''(x, y))$$

Putting in the limits of integration:

$$0 = \int_{-a}^a dx \tau(x) \int_{-a}^a dy (h'(x, y) - h''(s, y))$$

$$\tau(x) = \tau^2(x)$$

$$0 = \int_{-a}^a dx \tau(x) \int_{-a}^a dy (h'(x, y) - h''(s, y))$$

$$\tau(x) = \tau^2(x)$$

$$\tau(x) = \tau^2(x)$$

```
9   GOSUB 2000
10  MX(I,J) = (RAD*SL(I,J))/(2*LE)
11  IF IY(I,J)=0 THEN NX(I,J)=0:GOTO 100
12  I(I,J)=IY(I,J)
13  GOSUB 2000
15  NX(I,J) = (RAD*SL(I,J))/(2*LE)
100 NEXT J
105 NEXT I
106 PRINT "Starting to integrate m(x,y)"
110 H = RAD/HOR
130 REM Intergrate mx
180 FOR A = 1 TO HOR STEP 1
190 FOR J = 1 TO VRT STEP 1
196   S=MX(A,J)
200   FOR I = 2 TO HOR STEP 2
210     FOR CON = 1 TO 2 STEP 1
220       IF CON = 1 THEN S = S + 4*MX(I,J)
230       IF CON = 2 THEN S = S + 2*MX(I+1,J)
240     NEXT CON
250   NEXT I
260   M(A,J) = H * S / 3
270 NEXT J
275 NEXT A
276 REM Intergrate n(x,y)
277 H=RAD/VRT
280 PRINT "starting to integrate n(x,y)"
```

```
14 INPUT"Input the distance between the mirror and knife-edge";LE
15 INPUT"Input the number of points in x direction"; HOR
16 INPUT"Input the number of points in y direction"; VRT
18 INPUT "Input the background intensity"; IO
19 INPUT"Input radius of the mirror";RAD
20 REM Read Intensity in x direction
21 DIM IX(HOR,VRT),IY(HOR,VRT),MX(HOR,VRT),NX(HOR+1,VRT+1),P(VRT,HOR),G(HOR+1),
    F(VRT+1),M(HOR,VRT), N(HOR,VRT), ROY(VRT),ROX(HOR),H(HOR,VRT),FF(VRT+1),SL(V
    RT,HOR),I(VRT,HOR)
25 FOR I = 1 TO HOR
30     FOR J = 1 TO VRT
35         READ IX(I,J)
40     NEXT J
45 NEXT I
50 REM Read Intensity in y direction
55 FOR I = 1 TO HOR
60     FOR J = 1 TO VRT
65         READ IY(I,J)
70     NEXT J
75 NEXT I
80 REM Make transformation from intensity to slope of mirror
81 PRINT "Starting to calculate the slopes at each point on the mirror."
85 FOR I = 1 TO HOR
86     FOR J = 1 TO VRT
87 IF IX(I,J)=0 THEN MX(I,J)=0:GOTO 91
88 I(I,J)=IX(I,J)
```

APPENDIX A

Computer program to find the error in the surface of a mirror

The following computer program is written in Rising Star's version of Basic for the Epson QX-10 personal computer. The program reads the irradiance from the data file. The slope of both directions is then calculated and integrated. After an arbitrary function for $g(x)$ is chosen, an iteration is then set up and run to find the overall functions of each direction. Finally, the error in height is calculated and printed out.

The data file listed is from the case where it was assumed that the mirror had an height error function of

$h(x) = (x^2 - 2.5)$, where $x = (r/a)^2$ and a is the radius of the mirror. The program then finds the overall functions for

$u(x)$ and $v(x)$ and the difference between the starting point for the iteration and the final value of the function. For a perfect mirror the error in height would be zero across the entire surface.

checking out of mirrors in the infrared region, or examining microwave reflectors (antennae). And there are a vast number of possibilities in the visible region alone, for example, the automation of a lens/mirror grinding system, or the stabilization of a laser cavity. The basic design is the same for all cases, just a matter of proper scale.

Chapter 5

Conclusions and Recommendations

The work of this thesis has shown that all previous diffraction theory on the Foucault knife-edge test was inadequate to describe the actual results of the test. These inadequacies are: no bright ring is found around the image, no irradiance pattern is found outside of the mirror's boundary, coherent monochromatic light source does not produce a focogram, and that it is not the fields of the waves that add at the focal point but their intensity to produce a focogram. It has been shown that from the irradiance of the focogram, the error of the surface of the mirror can be detected and corrected. Also presented in this thesis are the design and major components comprising an adaptive optical system built around the Dall-Kirk test.

A possible factor in the discrepancy between the fine tuning of the computer code and the actual implementation into a control system, through use of the AD converter, is pointed out at the end of Chapter 4. The people responsible working on the AD converter should be contacted about the problem, as they are all in the same line of work. The programing discrepancy may be a result of the AD converter's limited word length.

The next step in the development of the adaptive system will be to use the computer to control the mirror's surface. This will require a more sophisticated control system than the one used in this thesis. The next step will be to use the computer to control the mirror's surface.

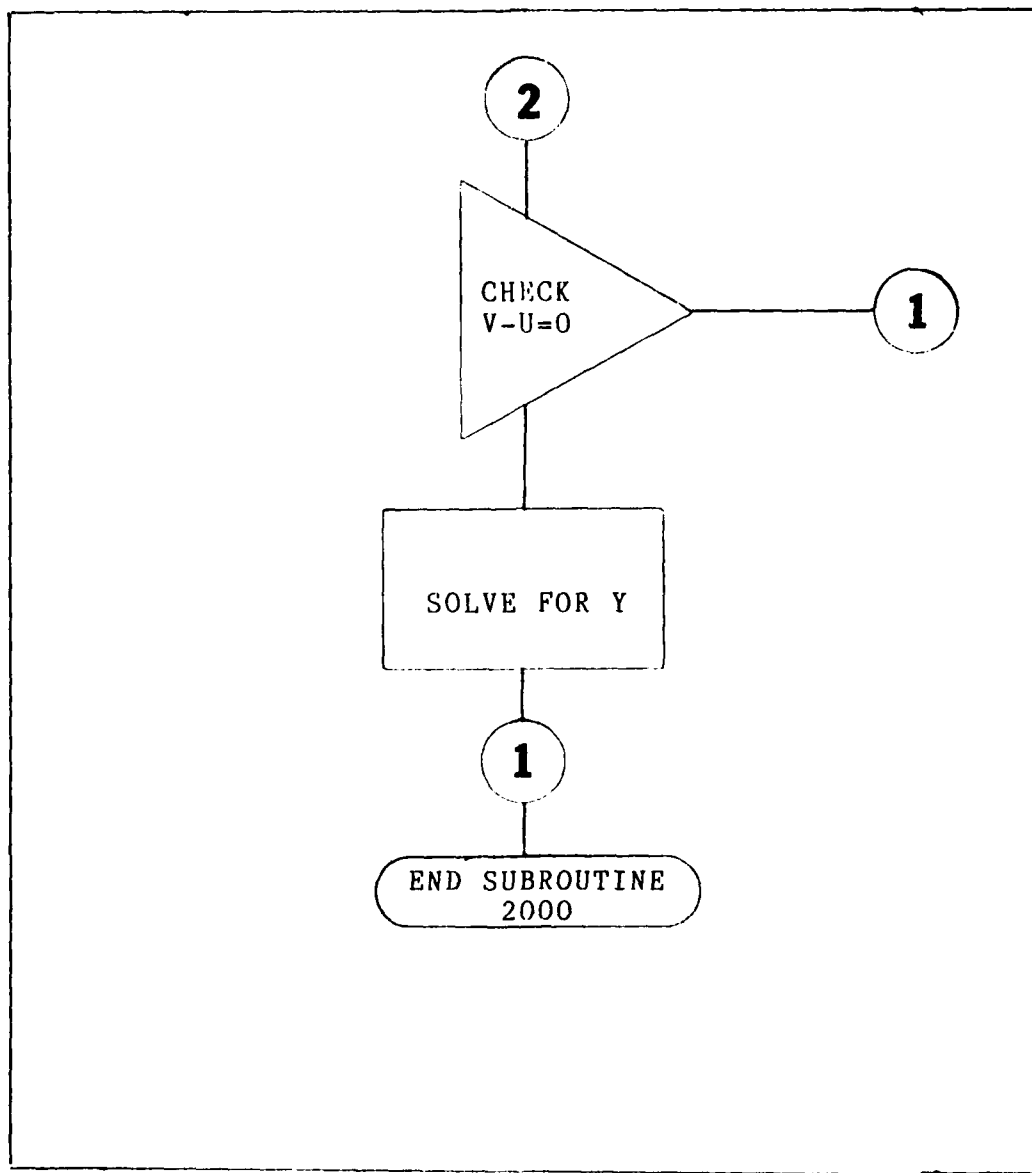


Figure 17d. The continuation of the flow chart.

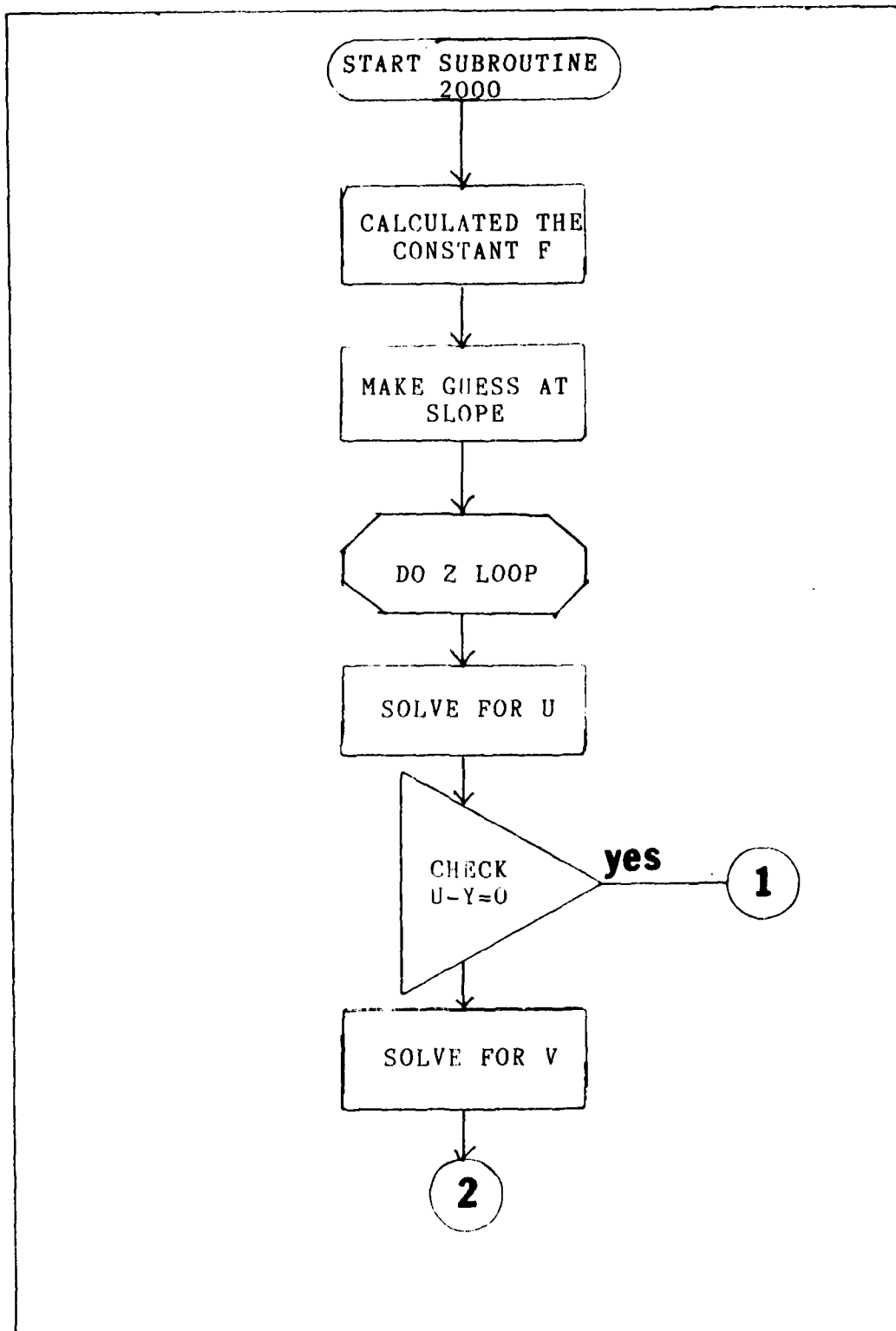


Figure 17c. The continuation of the flow chart.

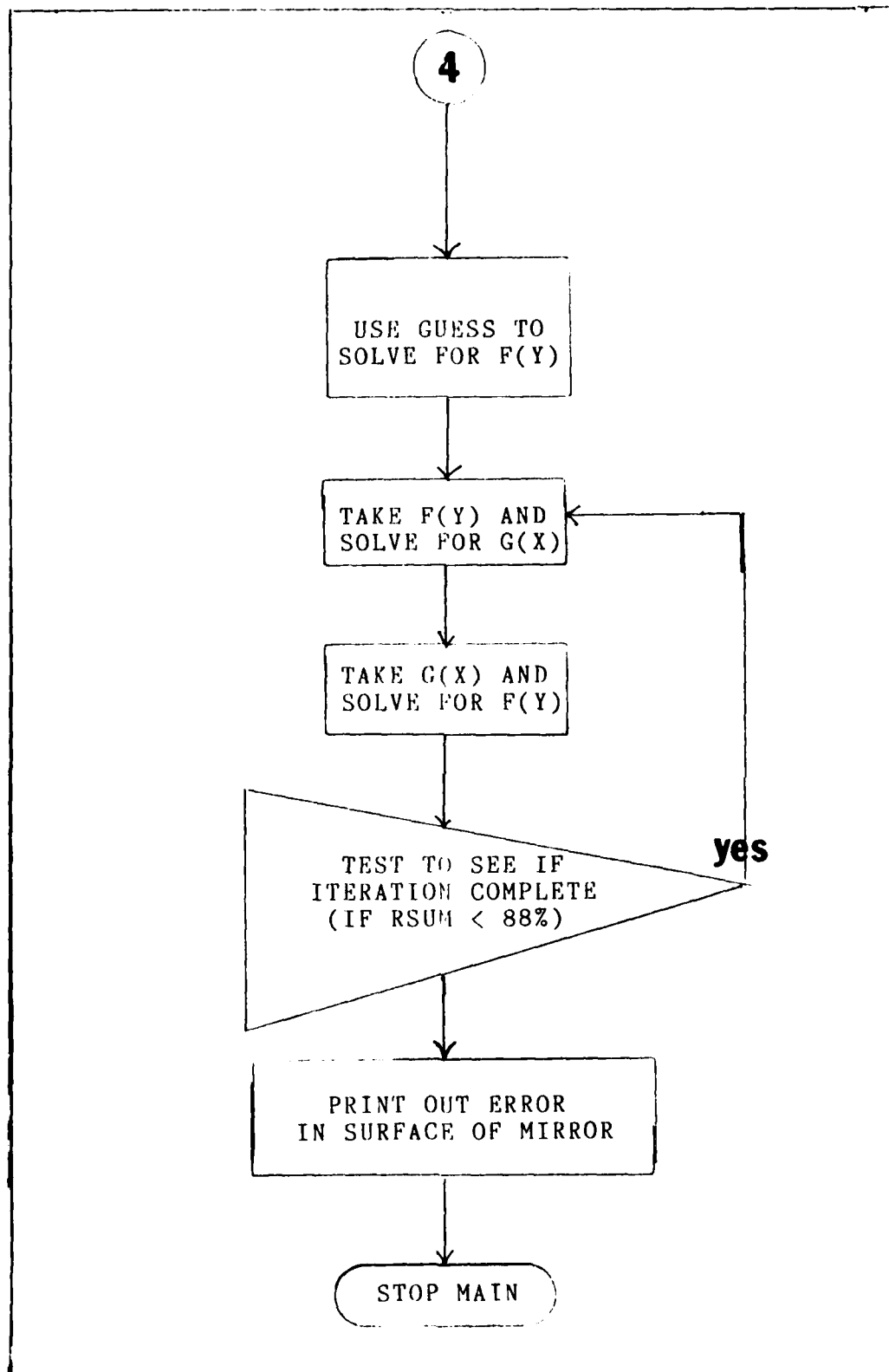


Figure 17b. The continuation of the flow chart.

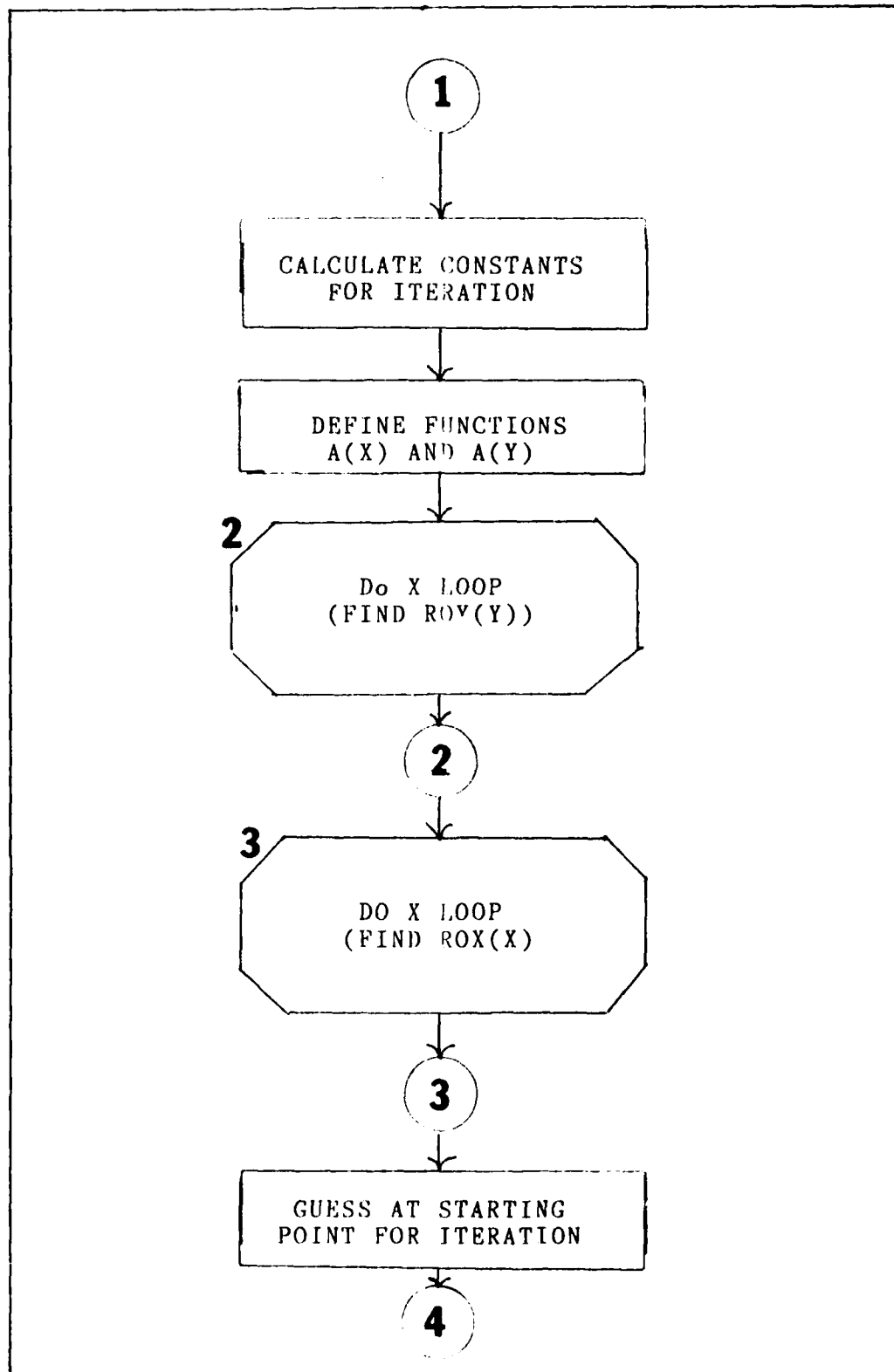


Figure 17a. The continuation of the flow chart.

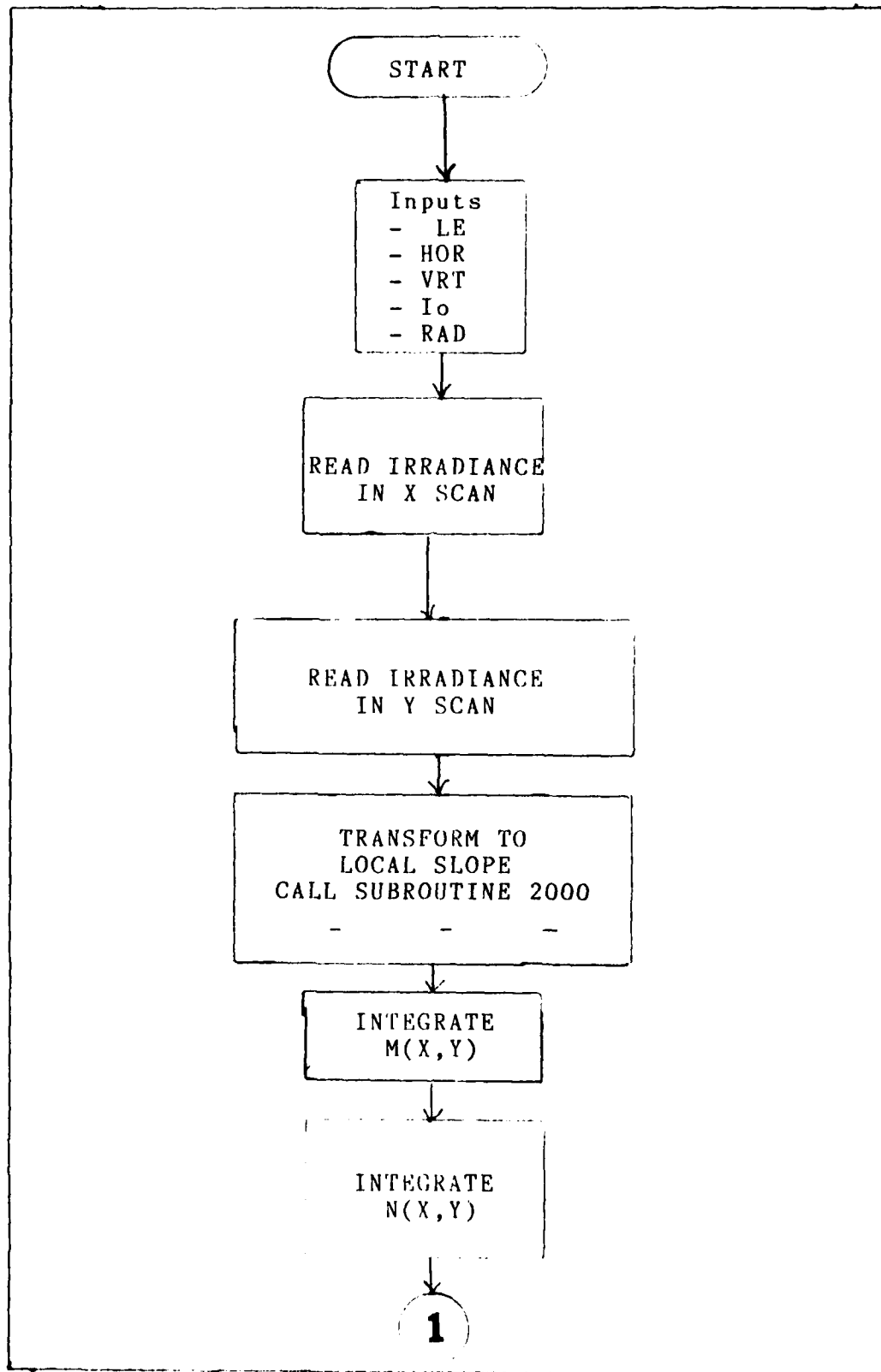


Figure 17. Flow chart of the computer program.

not using a system of this type because they are more concerned with wavefront sensing and controlling the wavefront on the out going wave, than with the surface of the mirror. They use fast acting actuators on the rear of the mirror to add imperfections to the wave front that cancel out the defects that occur during propagation to the target.

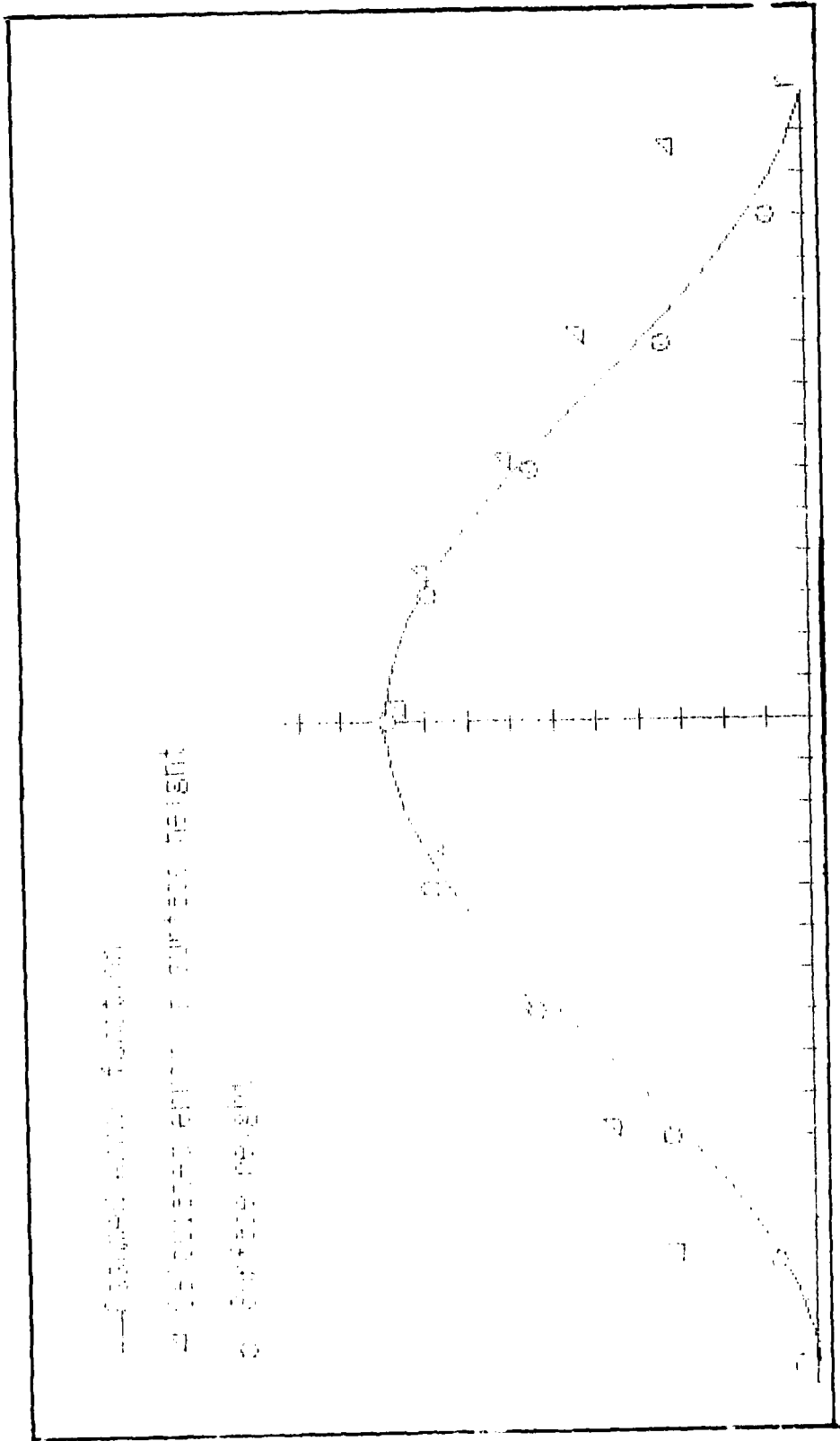


Figure 16. The graphed output across the mirror on the X-axis.

A computer program to solve for $h(x,y)$ from the above approach is included as appendix A. Appendix B is an output from a sample run. Figure 16 shows the graphed results along the x axis of a run where it was assumed the surface had an error function of $1 + \cos(\pi r/a)$, where a

was the radius and $r = (x^2 + y^2)^{1/2}$. The error function is represented as the solid curve. The height of the mirror at the points tested is shown as the circles, and the calculated error in the surface is shown as the triangles. The calculated error is close to the actual height except near the edge of the mirror. Upon closer examination of the computer code it was found (under the condition that this slight variation in surface height is due to the contribution made to the total error by the surface of the mirror's surface, which is not included in the model) is presented as follows:

The error in the height of the mirror is calculated by the computer program and is shown as the triangles in the graph. The error is close to the actual height except near the edge of the mirror.

As the program is run, the error in the height of the mirror is calculated by the computer program and is shown as the triangles in the graph. The error is close to the actual height except near the edge of the mirror.

The error in the height of the mirror is calculated by the computer program and is shown as the triangles in the graph. The error is close to the actual height except near the edge of the mirror.

$$0 = \int_{-a(x)}^{a(y)} dy (M(x,y) + f(y) - N(x,y) - g(x)) \text{ for any } x$$

$$0 = 2f(y)a(y) - \int_{-a(y)}^{a(y)} dx g(x) + \int_{-a(y)}^{a(y)} dx (M(x,y) - N(x,y))$$

$$0 = 2g(x)a(x) - \int_{-a(x)}^{a(x)} dy f(y) + \int_{-a(x)}^{a(x)} dy (M(x,y) - N(x,y))$$

$$\text{Let } p'(y) = \int_{-a(y)}^{a(y)} dx (M(x,y) - N(x,y)) \quad (4)$$

$$p''(x) = \int_{-a(x)}^{a(x)} dy (M(x,y) - N(x,y)) \quad (5)$$

$$f(y) = 1/2a(y) \left[p'(y) + \int_{-a(y)}^{a(y)} dx g(x) \right]$$

$$g(x) = 1/2a(x) \left[p''(x) + \int_{-a(x)}^{a(x)} dy f(y) \right]$$

The "1/2" is added to make the equations work.

$$M(x,y) = 1/2 [p'(y) + p''(x)] + f(y) + g(x)$$

$$\text{Now } p'(y) = \int_{-a(y)}^{a(y)} dx (M(x,y) - N(x,y)) \quad (6)$$

$$\text{and } p''(x) = \int_{-a(x)}^{a(x)} dy (M(x,y) - N(x,y)) \quad (7)$$

$$\text{and } f(y) = 1/2a(y) \left[p'(y) + \int_{-a(y)}^{a(y)} dx g(x) \right] \quad (8)$$

$$\text{and } g(x) = 1/2a(x) \left[p''(x) + \int_{-a(x)}^{a(x)} dy f(y) \right] \quad (9)$$

$$\text{and } M(x,y) = 1/2 [p'(y) + p''(x)] + f(y) + g(x) \quad (10)$$

```
290   FOR A = 1 TO VRT STEP 1
300   FOR I = 1 TO HOR STEP 1
306     S = NX(I,A)
310     FOR J = 2 TO VRT STEP 2
340       FOR CON = 1 TO 2 STEP 1
350         IF CON = 1 THEN S = S + 4 * NX(I,J)
360         IF CON = 2 THEN S =S + 2*NX(I,J+1)
370       NEXT CON
380     NEXT J
390     N(I,A) = H * S /3
395   NEXT I
396 NEXT A
397 REM Setting up constanst for the iterration phase.
400   FOR I = 1 TO HOR
410     FOR J = 1 TO VRT
420       P(I,J) = M(I,J) - N(I,J)
430     NEXT J
440   NEXT I
445 REM define functions a(y) and a(x)
450 DEF FN A(X) = SQR(RAD^2 -X^2)
460 DEF FN A(Y) = SQR(RAD^2 - Y^2)
465 REM solvinging the integrals for the constant functions of x and y
500   FOR Y=1 TO VRT STEP 1
505     S = P(1,Y)
510     FOR X = 1 TO (HOR/2-.5) STEP 2
530       S=S+4*P(X,Y)
```

```
540      S = S + 2*P(X+1,Y)
550      NEXT X
560      ROY(Y) = S*H/3
570 NEXT Y
620 FOR X=1 TO HOR
625   S=P(X,1)
630   FOR Y=2 TO (VRT/2-.5) STEP 2
640     S=S+4*P(X,Y)
650     S=S+2*P(X,Y+1)
660     NEXT Y
670     ROX(X)=S*H/3
680 NEXT X
685 REM Guess at what g(x) is, try 1-x^6
690 DEF FN G(X) = 1-(ABS(X))^6
695 DY = RAD/VRT
696 Y=0
699 REM Start point of iterration
700 FOR K = 1 TO VRT
710   Y=Y+DY
711   IF Y^2 => RAD^2 THEN GOTO 793
720   A=SQR(RAD^2-Y^2)
730   IN=0
740     FOR N=1 TO 11
750       X = -A + .2*A(N-1)
760       IN=IN+(.2*A)*FN G(X)
770     NEXT N
```

```
911 IF Y^2 => RAD THEN GOTO 992
920   A=SQR(RAD^2-Y^2)
930   IN=0
940   Z=INT(A/DX)
950   FOR N= 1 TO Z
960     IN=IN +DX*G(N)
970     NEXT N
980     FF(K)=(1/(2*A))*(ROY(K)+IN)
990   NEXT K
991 GOTO 997
992 FF(K)=0
993 GOTO 990
997 SUM=0
998   N=0
999 REM "Ready to check"
1000 FOR K= 1 TO HOR
1010   SUM=SUM+1
1020   DIF = FF(K)-F(K)
1030   IF DIF < 1E-03 THEN N=N+1
1040   F(K)=FF(K)
1050   NEXT K
1060   RSUM = N/SUM*100
1070   PRINT "The percent matched =",RSUM
1080   IF RSUM < 85 THEN 795
1090   REM if matched then print out f(y) and g(x) and find h(x,y)
991 FOR X = 1TO HOR
```

```
780 F(K)=(1/(2*A))*(ROY(K)+IN)
785 W=W
790 NEXT K
791 GOTO 795
793 F(K)= 0
794 GOTO 790
795 DX = RAD/HOR
796 X=0
799 REM "ready to start 800 loop"
800 FOR K = 1 TO HOR
810     X=X+DX
811 IF X^2 => RAD^2 THEN GOTO 893
820     A=SQR(RAD^2 - X^2)
830     IN=0
840     Z=INT(A/DY)
850     FOR N = 1 TO Z
860         IN =IN + DY*F(Z)
870     NEXT N
880 G(K) = 1/((2*A))*(ROX(K)+IN)
890 NEXT K
891 GOTO 899
893 G(K) = 0
894 GOTO 890
899 Y=0
900 FOR K=1 TO VRT
910     Y=Y+DY
```

```
992      PRINT F(X),G(X)
1093     NEXT X
1098     I=-1
1100     FOR X= 1 TO HOR
1105     J=-1
1110     FOR Y= 1 TO VRT
1115     IF (J^2+I^2) > RAD THEN H(X,Y)=0:GOTO 1130
1120     H(X,Y)=.5*(M(X,Y)+N(X,Y)+F(Y)+G(X))
1130     LPRINT X,Y,"Error is"H(X,Y)
1131     J=J+(2*(RAD/VRT))
1140     NEXT Y
1145     I=I+(2*(RAD/HOR))
1150     NEXT X
1160     GOTO 9999
1990     REM This is the subroutine to numericly solve for the slope of the mirror.
2000     F = I(I,J)/IO - PI/8
2100     Y=1E-03
2120     FOR Z = 1 TO 20
2200     U = SIN(F + SQR(ABS(1-Y*Y)))
2205     IF (U-Y) = 0 THEN GOTO 2300
2210     Y = 1/(U-Y)
2211     V=SIN(F+U*SQR(1-U*U))
2212     IF (V-U) = 0 THEN V=Y; GOTO 2300
2213     V=1/(V-U)
2214     IF (V-Y) = 0 THEN GOTO 2300
2215     Y=U+1/(V-Y)
```


APPENDIX B A SAMPLE OUTPUT FROM PROGRAM

	1	Error is 0
1	2	Error is 0
1	3	Error is 0
1	4	Error is 0
1	5	Error is 0
1	6	Error is 0
1	7	Error is 0
1	8	Error is 0
1	9	Error is 0
1	10	Error is 0
1	11	Error is 0
2	1	Error is 0
2	2	Error is 0
	3	Error is 0
2	4	Error is 1.1384639849
2	5	Error is 1.1372537323
2	6	Error is 1.1388195447
2	7	Error is 1.137878966
2	8	Error is 1.1374952983
2	9	Error is 1.1380261465
2	10	Error is 0
2	11	Error is 0
3	1	Error is 0
3	2	Error is 0
3	3	Error is 1.1388024637
3	4	Error is 1.1396093156

3	5	Error is 1.1383997087
3	6	Error is 1.1399658315
3	7	Error is 1.1390248203
3	8	Error is 1.1386402233
3	9	Error is 1.1391705686
3	10	Error is 1.1364436818
3	11	Error is 0
4	1	Error is 0
4	2	Error is 1.1399686284
4	3	Error is 1.1405416143
4	4	Error is 1.1413486153
4	5	Error is 1.140138311
4	6	Error is 1.1417042413
4	7	Error is 1.1407631514
4	8	Error is 1.140378128
4	9	Error is 1.1409084712
4	10	Error is 1.1381820315
4	11	Error is 1.1151828256
5	1	Error is 0
5	2	Error is 1.1407981127
5	3	Error is 1.1413812201
5	4	Error is 1.1421781141
5	5	Error is 1.140966361
5	6	Error is 1.1425316291
5	7	Error is 1.1415906985
5	8	Error is 1.141205673
5	9	Error is 1.1417364446

5	10	Error is 1.1390109322
5	11	Error is 1.1160117263
6	1	Error is 0
6	2	Error is 1.1442853743
6	3	Error is 1.1448593163
6	4	Error is 1.1456654273
6	5	Error is 1.1444530782
6	6	Error is 1.146018696
6	7	Error is 1.1450772066
6	8	Error is 1.1446920279
6	9	Error is 1.1452228761
6	10	Error is 1.1424977963
6	11	Error is 1.1194985905
7	1	Error is 0
7	2	Error is 1.1402571981
7	3	Error is 1.1408306952
7	4	Error is 1.1416367275
7	5	Error is 1.1404245377
7	6	Error is 1.1419895967
7	7	Error is 1.1410488752
7	8	Error is 1.1406642864
7	9	Error is 1.1411953954
7	10	Error is 1.1384700051
7	11	Error is 1.1154707992
8	1	Error is 0
8	2	Error is 1.1388769069

8	3	Error is 1.1394494872
8	4	Error is 1.1402550931
8	5	Error is 1.1390429011
8	6	Error is 1.140607807
8	7	Error is 1.1396676754
8	8	Error is 1.1392846058
8	9	Error is 1.1398163441
8	10	Error is 1.13709031
8	11	Error is 1.1140911041
9	1	Error is 0
9	2	Error is 1.140134488
9	3	Error is 1.1407066998
9	4	Error is 1.1415123037
9	5	Error is 1.1403005402
9	6	Error is 1.1418655226
9	7	Error is 1.1409256518
9	8	Error is 1.1405432114
9	9	Error is 1.1410748048
9	10	Error is 1.138347918
9	11	Error is 1.1153487121
10	1	Error is 0
10	2	Error is 0
10	3	Error is 1.1330263727
10	4	Error is 1.1338326099
10	5	Error is 1.1326217736
10	6	Error is 1.1341871886

Bibliography

1. Aldrich, Dr. Ralph E. Personal correspondence and telephone interview. ITEK Optical Systems, 10 Maguire Road, Lexington, Massachusetts, 02173. July, 1984.
2. Banerji, Subhansukumar. "On Some Phenomena Observed in the Foucault Test". Astrophysical Journal. Volume 48, pages 56-58. 1918.
3. Barakat, Richard. "General Diffraction Theory of Optical Aberration Tests, from the Point of View of Spatial Filtering". Journal of the Optical Society of America. Volume 59, Number 11. Pages 1432-1433. November 1969.
4. Barakat, Roub. Image Registration for Peak Evaluation of Analytical Electron Spectroscopy. PhD dissertation. The University of Arizona. 1979.
5. Bendat, Julian S., and Piersol, Allen G. Engineering Analysis of Random Signals and Noise. Wiley and Sons, New York, 1971.
6. Perry, Mark W. Ph.D. Thesis, Department of Electrical Engineering, University of Arizona. 1981. Ph.D. Thesis, Department of Electrical Engineering, University of Arizona. 1981. Ph.D. Thesis, Department of Electrical Engineering, University of Arizona. 1981.

7. Cox, R. E. and Sinnott, R. W. "Glennings for AD's". Sky and Telescope, Volume 52. Number 3. pages 212-216 September 1976.

8. Dall, H. E. "A Null Test for Paraboloids". The Journal of the British Astronomical Association. Pages 149-155. Volume 57, Number 5. 1947.

9. Dodgen, Dave. "Testing of Convex Paraboloids". Optical Engineering. Volume 14, Number 6. Pages 526-528. November-December 1975.

10. Fournelle, L. M. "Description des Procédés Employés pour le Contrôle de Qualification des Surfaces Optiques". C. R. Acad. Sci. Paris, Volume 43, page 504, 1956. (It printed in Glennings de L. Sinnott, Volume 28, B, Second Coll.)

11. Fournelle, L. M. "Méthodes pour la Construction des Téléscopes paraboliques". Revue de l'Optique, Paris, Volume 5, page 197, 1956.

12. Fournelle, L. M. "Méthodes pour la Construction des Téléscopes paraboliques". Revue de l'Optique, Paris, Volume 5, page 197, 1956.

13. Fournelle, L. M. "Méthodes pour la Construction des Téléscopes paraboliques". Revue de l'Optique, Paris, Volume 5, page 197, 1956.

14. Gaskill, Jack D. Linear Systems, Fourier Transforms, and Optics. New York, John Wiley & Sons. 1978.
15. Gatewood, B. E. Comparison of Various Methods of Mathematical Analysis of the Foucault Knife-Edge Test Pattern to Determine Optical Imperfections. Contract No. NGR-36-008-153. The Ohio State University Research Foundation, Columbus, Ohio. for Langley Research Center. NASA CR-1906. November 1971. (AD D300411)
16. Goodman, Joseph W. Introduction to Fourier Optics. San Francisco, McGraw-Hill Book Company. 1968.
17. Gradshteyn, I. S. and Ryzhik, I. M. Table of Integrals, Series, and Products. Corrected and Enlarged Edition. Translated from the Russian by Scripta Technica, Inc., and edited by Alan Jeffrey. New York, Academic Press. 1980.
18. Hansen, Major James Gerald Raymond. Structural Design of a large Deformable Primary Mirror for a Space Telescope. The University of Arizona. May 1981. (AD-A107-260).
19. Hansler, R. L. "A Holographic Foucault Knife-edge Test for Optical Elements of Arbitrary Design." Applied Optics. Volume 7, Number 9. Pages 1863-1864. September 1968.
20. Holleran, Robert T. "An Algebraic Solution for the Small Null Compensator." Applied Optics. Volume 7, Number 1. January 1968. Pages 137-144.

21. Ingalls, Albert G. Editor. Amateur Telescope Making (Book Three). Kingsport, Tennessee: Kingsport Press, Inc. 1953.
22. Katzoff, Samuel. Quantitative Determination of Optical Imperfections by Mathematical Analysis of the Foucault Knife-Edge Test Pattern. NASA Langley Research Center, Hampton, Va. NASA TN D-6119. August 1971. (AD D300314)
23. Kocher, David G. "Automated Foucault test for focus sensing." Applied Optics. Volume 22, Number 12. Pages 1887-1892. 15 June 1983.
24. Linfoot, E. H. Recent Advances in Optics. Oxford University Press, Amen House, London, England. 1955.
25. Longair, Malcolm S. "The Space Telescope and its Capabilities," Proceedings of ESA/ESO Workshop on Astronomical Uses of the Space Telescope. 5-26 February 1979
26. Malacara, Daniel; editor. Optical Shop Testing. John Wiley and Sons, New York. 1978.
27. Masterson, Keith and Lind, M. Matrix Approach for Testing Mirrors-Part 1. Solar Energy Research Institute. Golden, Colorado. Operated for the U.S. Department of Energy under contract No. EG-77-C-01-4042. April 1983.
28. Rayleigh, Lord Baron. O.M., D.Sc., F.R.S. Scientific Papers. Cambridge University Press, London, England. Volume VI. 1911-1919.

29. Robertson, Hugh J. Development of an Active Optics Concept Using a Thin Deformable Mirror. NASA CR-1593. The Perkin-Elmer Corporation, Norwalk, Conn. for the Langley Research Center. 17 August 1970.
30. Sinnott, Roger W. "Gleanings for ATM's. 'Surface Profile From the Foucault Test'." Sky and Telescope. Pages 519-522. May 1982.
31. Texereau, Jean. How to Make a Telescope. Translated and Adapted from the French by Allen Strickler. Interscience Publishers, Inc., New York. 1957.
32. Ward, James C. Jr. (Compiled by). Large Space Systems Technology-1979. Compiled reports of the First Annual Program Technical Review held at NASA Langley Research Center Hampton, Virginia, November 7-8, 1979. NASA Conference Publication 2118. 1980.
33. Welford, W. T. "A Note on the Theory of the Foucault Knife-edge Test". Optics Communications. Volume 1, Number 9, April 1970. Pages 443-445.
34. Wilford, John Noble. "Mishaps May Delay a Space Telescope." The New York Times. page 28. column 1. 13 February 1984.

35. Wilson, R. Gale. "Wavefront-error Evaluation by Mathematical Analysis of Experimental Foucault-test Data." Applied Optics. Volume 14, Number 9. Pages 2286-2297. September 1975.

36. Zernike, F. (communicated by Professor F. J. H. Stratton). "Diffraction Theory of the Knife-edge Test and its Improved Form, The Phase-Contrast Method". Royal Astronomical Society Monthly Notices. Volume 94, pages 377-399. 1934b.

VITA

Captain Randy L. Wingler was born on 3 April 1958 in Shell Lake, Wisconsin. He graduated from Spooner High School, Spooner, Wisconsin, in 1976 and attended the University of Wisconsin-Superior from which he received the degree of Bachelor of Science in Physics in May 1980. Upon graduation he received a commission in the USAF through the ROTC program. He was then called to active duty Aug 80 and reported to Hill AFB, Utah. There he served two and half years as the manager of the Photoreconnaissance Engineering Test Facility until entering the School of Engineering, Air Force Institute of Technology, WPAFB, Ohio, in June 1983.

Permanent address: Route 1, Box 59

Sarona, Wisconsin 54870

REPORT DOCUMENTATION PAGE

1. REPORT SECURITY CLASSIFICATION unclassified		1b. RESTRICTIVE MARKINGS	
2a. SECURITY CLASSIFICATION AUTHORITY		3. DISTRIBUTION STATEMENTS (When Applicable) (See Instructions on Reverse Side) <i>Unlimited Distribution</i> Approved for public release: IAW AFR 190-17. LYNN E. WOLAVER Dean for Research and Professional Development Air Force Institute of Technology (AFIT) and Professional Development Wright-Patterson AFB OH 45433	
2b. DECLASSIFICATION/DOWNGRADING SCHEDULE		5. MONITORING ORGANIZATION REPORT NUMBER(S) 45433	
4. PERFORMING ORGANIZATION REPORT NUMBER(S) AFTT/CEP/PH/84D-14		7a. NAME OF MONITORING ORGANIZATION	
6a. NAME OF PERFORMING ORGANIZATION School of Engineering Air Force Institute of Technology	6b. OFFICE SYMBOL (If applicable) AFIT/CEP	7b. ADDRESS (City, State and ZIP Code)	
6c. ADDRESS (City, State and ZIP Code) Wright-Patterson AFB, Ohio 45433		9. PROCUREMENT INSTRUMENT IDENTIFICATION NUMBER	
8a. NAME OF FUNDING/SPONSORING ORGANIZATION	8b. OFFICE SYMBOL (If applicable)	10. SOURCE OF FUNDING NOS.	
8c. ADDRESS (City, State and ZIP Code)		PROGRAM ELEMENT NO.	TASK NO.
11. TITLE (Include Security Classification) See Box 19		PROJECT NO.	WORK UNIT NO.
12. PERSONAL AUTHOR(S) Randy L. Wiegler, M.S., Capt, USAF			
13a. TYPE OF REPORT MS Thesis	13b. TIME COVERED FROM _____ TO _____	14. DATE OF REPORT (Yr., Mo., Day) 1984 December	15. PAGE COUNT 73
16. SUPPLEMENTARY NOTATION			
17. COSATI CODES		18. SUBJECT TERMS (Continue on reverse if necessary and identify by block number)	
FIELD	GROUP	Adaptive Optics, Space Telescope, Telescope, Foucault	
	SUB. GR.	Test, Ball-Null Test, Testing	
19. ABSTRACT (Continue on reverse if necessary and identify by block number)			
Title: Ball-Null Tester for Spaceborne Applications Thesis Advisor: Dr. Donn Shankland			
20. DISTRIBUTION/AVAILABILITY OF ABSTRACT UNCLASSIFIED/UNLIMITED <input checked="" type="checkbox"/> SAME AS RPT. <input type="checkbox"/> DTIC USERS <input type="checkbox"/>		21. ABSTRACT SECURITY CLASSIFICATION UNCLASSIFIED	
22a. NAME OF RESPONSIBLE INDIVIDUAL Dr. Donn Shankland		22b. TELEPHONE NUMBER (Include Area Code) (513) 255-2012	22c. OFFICE SYMBOL AFTT/CEP

Approved for public release: IAW AFR 190-17.
LYNN E. WOLAVER *Lynn Wola*
Dean for Research and Professional Development
Air Force Institute of Technology (AFIT)
Wright-Patterson AFB OH 45433

Abstract

This is a study to design a self correcting primary mirror system for a space telescope. The design is centered around a Dall-Null tester (a Foucault knife-edge tester with compensating lens). An indepth study of the theory of the Foucault test from Foucault's original publications to current work is presented. Also short comings of the diffraction approach are shown. The findings of an simple experiment showed the way to the correct explanation as to the workings of the test. Based on this new explanation, a computer program to find the error in the surface of the mirror from the irradiance pattern provided by the Dall-Null tester was developed. The computer program with a sample run is included in the appendixes A and B.

The basic design of an adaptive optic system for a space-borne application is also presented in the paper. This design has the desired quality of being able to correct the mirror while the telescope is in use. The equations being independent of wavelength allows for the design to be applied to systems working outside of the visible spectrum as well as the systems working in the visible.

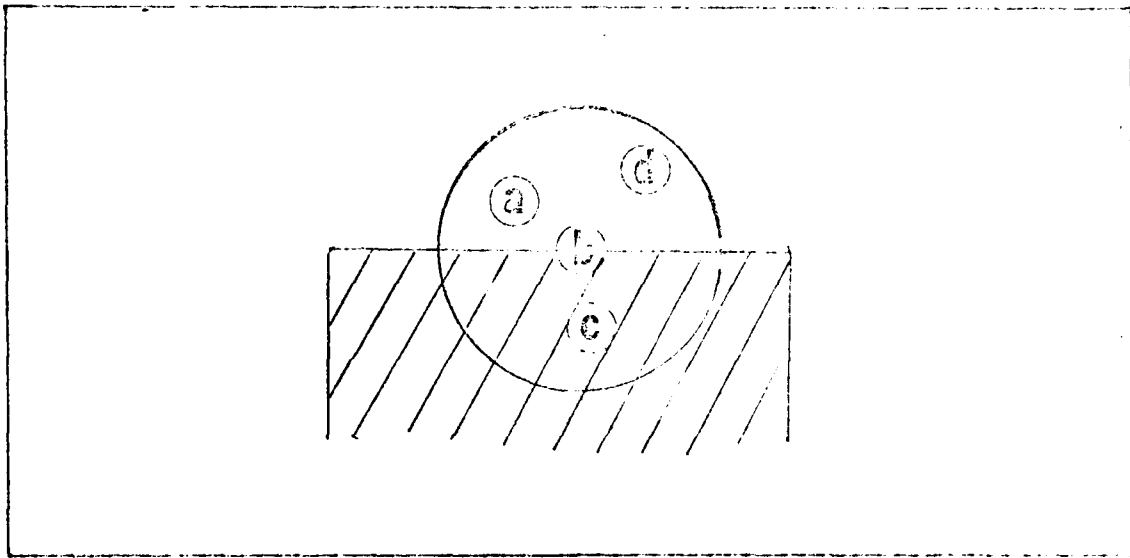


Figure 6. The relative position of the Arty patterns at the knife-edge.

image, cases a and d, then all of the image will pass the knife-edge. But if the slope lowered the image, case c, the knife-edge would cut it off completely. Thus the irradiance of the resulting image would be determined by how much of each segment's image was passed by the knife-edge. Figure 7 shows the result for the current situation.

Thus the correct theory of the Foucault test is revealed, and likewise, so is the theory of the Bill-Hall test. And in chapter four this theory will be put to work to find the error in the height of the mirror surface.

END

FILMED

11-85

DTIC